SANDIA REPORT

SAND2016-4856
Unlimited Release
Printed May 2016

Analysis of PV Advanced Inverter Functions and Setpoints under Time Series Simulation

John Seuss, Matthew J. Reno, Robert J. Broderick, Santiago Grijalva

Prepared by
Sandia National Laboratories
Albuquerque, New Mexico 87185 and Livermore, California 94550

Sandia National Laboratories is a multi-program laboratory managed and operated by Sandia Corporation, a wholly owned subsidiary of Lockheed Martin Corporation, for the U.S. Department of Energy's National Nuclear Security Administration under contract DE-AC04-94AL85000.

Issued by Sandia National Laboratories, operated for the United States Department of Energy by Sandia Corporation.

Available to DOE and DOE contractors from
U.S. Department of Energy
Office of Scientific and Technical Information
P.O. Box 62
Oak Ridge, TN 37831

Telephone: (865) 576-8401
Facsimile: (865) 576-5728
E-Mail: reports@adonis.osti.gov
Online ordering: http://www.osti.gov/bridge

Available to the public from
U.S. Department of Commerce
National Technical Information Service
5285 Port Royal Rd.
Springfield, VA 22161

Telephone: (800) 553-6847
Facsimile: (703) 605-6900
E-Mail: orders@ntis.fedworld.gov
Online order: http://www.ntis.gov/help/ordermethods.asp?loc=7-4-0#online

SAND2016-4856
Unlimited Release
Printed May 2016

Analysis of PV Advanced Inverter Functions and Setpoints under Time Series Simulation

Matthew J. Reno, Robert J. Broderick
Photovoltaics and Distributed Systems Integration
Sandia National Laboratories
P.O. Box 5800
Albuquerque, New Mexico 87185-1033

John Seuss, Santiago Grijalva
School of Electrical and Computer Engineering
Georgia Institute of Technology
777 Atlantic Drive NW
Atlanta, GA 30332-0250

Abstract

Utilities are increasingly concerned about the potential negative impacts distributed PV may have on the operational integrity of their distribution feeders. Some have proposed novel methods for controlling a PV system's grid-tie inverter to mitigate potential PV-induced problems. This report investigates the effectiveness of several of these PV advanced inverter controls on improving distribution feeder operational metrics. The controls are simulated on a large PV system interconnected at several locations within two realistic distribution feeder models. Due to the time-domain nature of the advanced inverter controls, quasi-static time series simulations are performed under one week of representative variable irradiance and load data for each feeder. A parametric study is performed on each control type to determine how well certain measurable network metrics improve as a function of the control parameters. This methodology is used to determine appropriate advanced inverter settings for each location on the feeder and overall for any interconnection location on the feeder.

CONTENTS

FIGURES

TABLES

NOMENCLATURE

ANSI	American National Standards Institute
CPUC	California Public Utilities Commission
COM	Component Object Model
DOE	Department of Energy
EPRI	Electric Power Research Institute
IEEE	Institute of Electrical and Electronics Engineers
LDC	load duration curve
MW	Megawatts (AC)
NREL	National Renewable Energy Laboratory
OpenDSS	Open Distribution System Simulator™
PCC	Point of Common Coupling
PF	power factor
pu	per unit
PV	Photovoltaic
QSTS	Quasi-Static Time Series
SCADA	Supervisory Control and Data Acquisition

1. INTRODUCTION

With the increasing adoption of photovoltaic (PV) generation in distribution networks, utilities are becoming ever more cautious about the impacts PV may have on network operation and maintenance. Research has shown that PV installation sizes must be limited to prevent them from causing voltage deviation and line overcurrent violations [1-3]. It has also been shown that the variability of PV generation can have a negative impact on the operation of voltage regulators and switching capacitors [4, 5]. A PV system's impact on voltage regulating equipment also affects whether or not line voltages remain within ANSI limitations. For this reason, a potential PV installation must be studied using quasi-static time series (QSTS) simulations to capture how the predicted variability of the PV generation and network load affect existing voltage regulation controls. If the study of a particular PV interconnection shows a significant increase in the operation of network equipment or voltage deviations, then the interconnection will be denied.

However, it has also been shown that the PV system's grid-tie inverter can be utilized to ensure the PV system's variability does not cause a significant negative impact to the distribution network. Specifically, so-called "Advanced Inverter" functionalities in modern inverters have been proposed to this end [6, 7]. Since there is an increasing number of PV inverter manufacturers, a standard set of control functions is being proposed by the California Public Utilities Commission (CPUC) that all inverter manufacturers must provide in order to be approved for use on California distribution networks. Advanced inverter functions can refer to a number of hardware and software capabilities, from the ability of the inverter to transmit data and receive new operating set-points to the ability to provide a certain amount of reactive power or curtail the power output of the PV system to desired level. Although there are currently no recommended uses for advanced inverter controls, these standard functions will provide utilities the flexibility to select the PV system behavior that best suits any given scenario.

The problem that is addressed by this research is that the advanced inverter functionalities, and in particular the advanced inverter controls which dictate the real and reactive power output of the PV system based on local measurements, may not necessarily improve the impact of the PV system on the distribution network. In fact, this research will show that there are certain control settings that will result in the PV system causing more problems than if it had no advanced inverter controls at all. Some poor settings may be obvious, such as instructing the PV inverter to output a large amount of capacitive vars while at high line voltages will cause more over-voltage scenarios than the PV system with no control. However, situations such as the injection of a certain amount of reactive power during a period of highly variable irradiance and the impact it has on voltage regulator tap changes are less obvious and must be simulated to determine if there is an overall improvement or not. Additionally, depending on the interconnection location of the PV system, it may not even have enough of a measurable negative impact on the network to even warrant certain control types.

The goal of this research is to determine the appropriate advanced inverter control parameters that will provide an overall improvement in the operation of the distribution network compared to the PV under "legacy" control, or simply outputting all real power available to it at unity power factor. Only advanced inverter controls that can be simulated in a QSTS simulation are studied. These controls are summarized in Section 2 along with the other QSTS simulation details. Section 3 introduces the test feeders and demonstrates the impact of PV on them. It then goes on to describe how network measurements are used to find the acceptable range of inverter controls for each PV interconnection location. Example results of each control using one week of representative load and irradiance data

are presented in Section 4. The acceptable range of control parameters for each control type are generalized for each feeder studied in Section 5. Finally, conclusions are drawn and further research is suggested in Section 6.

2. MODELING ADVANCED INVERTER FUNCTIONS

2.1. Advanced Inverter Functions Considered

This section lists the advanced inverter control types considered in this research, briefly describes them, and indicates which variable parameters are to be considered. Six advanced inverter controls are selected from the set under consideration by CPUC in [7] based on their ability to be simulated in the OpenDSS QSTS simulation environment. For each of control's parameters, the units are given in parentheses and the range of parameters considered is given in brackets. The parameters have been selected and defined to minimize the total number of parameters necessary to define the control action. This is due to the fact that each additional parameter increases the dimensionality of the problem and thus geometrically increases the computation time required. At the end of this section, the network metrics used to determine the successfulness of each control are described.

2.1.1. Ramp-Rate Control

This function limits the up-ramp of the PV systems to a fixed rate over time. The down-ramp is not limited since the PV system cannot store energy. A lower parameter value in this case means there is a greater amount of PV power curtailment due to output limiting. At the lowest parameter tested, the PV will only be allowed to increase its output level by a tenth of its rating in an hour.

Parameters:

- Ramp-rate limit ($P_{PV,p.u.}/hr$) [0.1 – 1.5]

2.1.2. Fixed Power Factor Control

This function sets the inverter to operate at a constant power factor. This means as the PV real power output increases, the reactive power output will increase proportional to the power factor. For this reason, only lagging (negative) power factors are considered to prevent voltage rise associated with PV system output. However, if the inverter is not large enough, it will only output the reactive power available to it and not curtail the real power.

Parameters:

- Power factor (pf) [(-0.99) – (-0.7)]

2.1.3. Volt/Watt Control

This function controls the PV inverter using a similar voltage-based droop curve as in Figure 1, but curtails the real power output as voltage becomes too high, rather than dispatch Vars. Since it operates only in the region of $V_{p.u.} > 1.0$, the deadband starts at nominal and the PV output is curtailed based on the steepness of the slope past that.

Parameters:

- Volt/Watt slope ($\Delta P_{p.u.}/\Delta V_{p.u.}$) [5 – 100]
- Deadband width (V_{pu}) [0-.04]

2.1.4. Watt-Triggered Power Factor Control

This function is similar to the previous except the power factor becomes more lagging as the real power output increases based on a defined slope. This means as the real power ramps from zero to peak output, the power factor changes from unity to a maximum lagging value, the target power factor at rated output. Again, the real power output is prioritized if the inverter is not large enough to supply the necessary vars.

Parameters:

- Target power factor (pf) [0.7 – 0.99]
- Deadband width ($P_{PV,p.u.}$) [0.9 – 0]

2.1.5. Watt-Priority Volt/Var Control

This function outputs reactive power from the PV grid-tie inverter based on a droop slope with a deadband around nominal voltage, such as in Figure 1. The vertical axis for this control is available reactive power, or $Q_{avail} = \sqrt{S_{inv}^2 - P_{PV}^2}$, where S_{inv} is the rating of the inverter and P_{PV} is the real power available to the PV system from the irradiance. The control will have the inverter output all available real power before dispatching reactive power based on the measured local voltage.

Parameters:

- Volt/Var droop slope ($\Delta Q_{avail,p.u.}/\Delta V_{p.u.}$) [5 – 100]
- Deadband width (V_{pu}) [0 – 0.04]
- Target voltage (V_{pu}) [0.98 – 1.03]

2.1.6. Var-Priority Volt/Var Control

This function outputs reactive power from the PV grid-tie inverter similar to the previous control, but instead limits the real power based on the reactive power needs, or $P_{PV} = \sqrt{S_{inv}^2 - Q_{Volt/Var}^2}$. In this case, the vertical axis of Figure 1 is the full rating of the inverter. This control will actually curtail the real power output of the PV if there is not enough inverter capacity to provide enough Vars to regulate voltage based on the droop curve.

Parameters:

- Volt/Var droop slope ($\Delta Q_{avail,p.u.}/\Delta V_{p.u.}$) [5 – 100]
- Deadband width (V_{pu}) [0-.04]

- Target voltage (V_{pu}) [0.98-1.03]

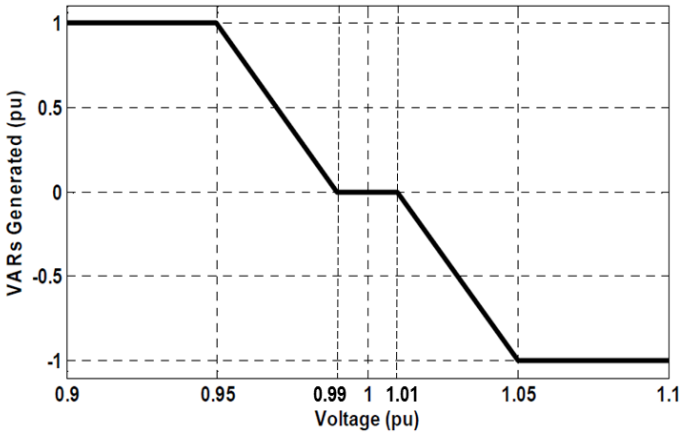

Figure 1. Example Volt/Var droop curve with a slope of 25$\Delta Q/\Delta V$ and a deadband of width 0.02V.

2.2. Example Simulations Demonstrating Advanced Inverter Functions

This subsection presents the methodology used to simulate PV inverters in quasi-steady-state time-series (QSTS) simulations. The simulation platform is OpenDSS, which is operated via Matlab in conjunction with the Sandia GridPV toolbox [8].

2.2.1. Weekly Irradiance, Load Selection, and Basecase Simulation

To demonstrate the controls described in the previous section, a time-series simulation must be run in order to see how the controls react to fluctuations in load, irradiance, and other network controllers. Since the local inverter controls are assumed to be stable and converge faster than the 1-minute load and irradiance data available, a QSTS simulation is appropriate. For initial demonstration of the advanced inverter controls in Section 2.2, feeder CO1 is used. A year of substation SCADA data collected at 1-minute resolution was allocated to model the variations in feeder load throughout the year. Irradiance data from the University of California San Diego was used to model a fixed-tilt PV system with appropriate smoothing for a large central plant [9]. A representative week of irradiance data was selected and paired with a representative week of load to use as a basis for the QSTS analysis. The representative week was chosen by identifying the week of load that minimized the square of the error between its load duration curve (LDC) and the yearly LDC, as shown in Figure 2. This process resulted in the load and irradiance data shown in Figure 3, which are used as the basis for the QSTS analysis. It should be noted that the reactive power measurements in Figure 3 are assumed to be bad data due to their shape and have therefore been discarded. The real power curve is allocated to each network load which are then held at a given power factor.

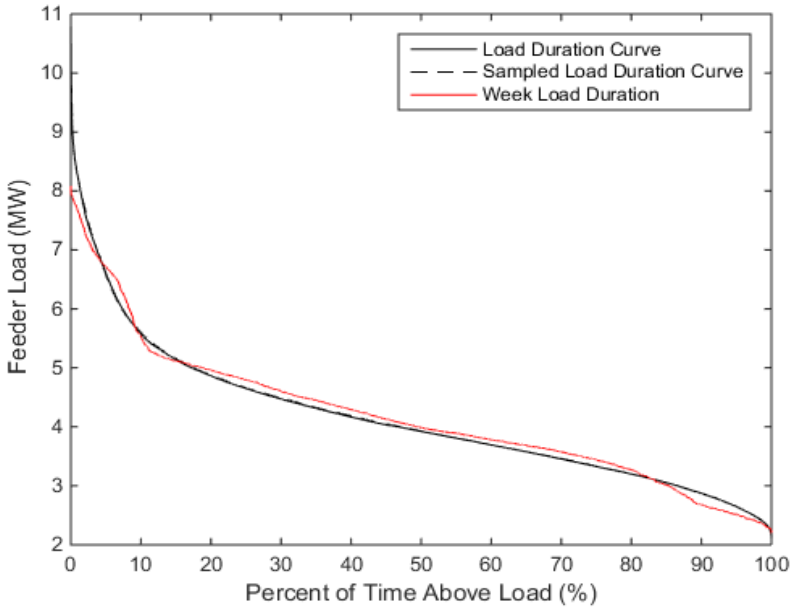

Figure 2. Weekly load selected for QSTS simulation's LDC selected as the least-square-error of the yearly data's LDC.

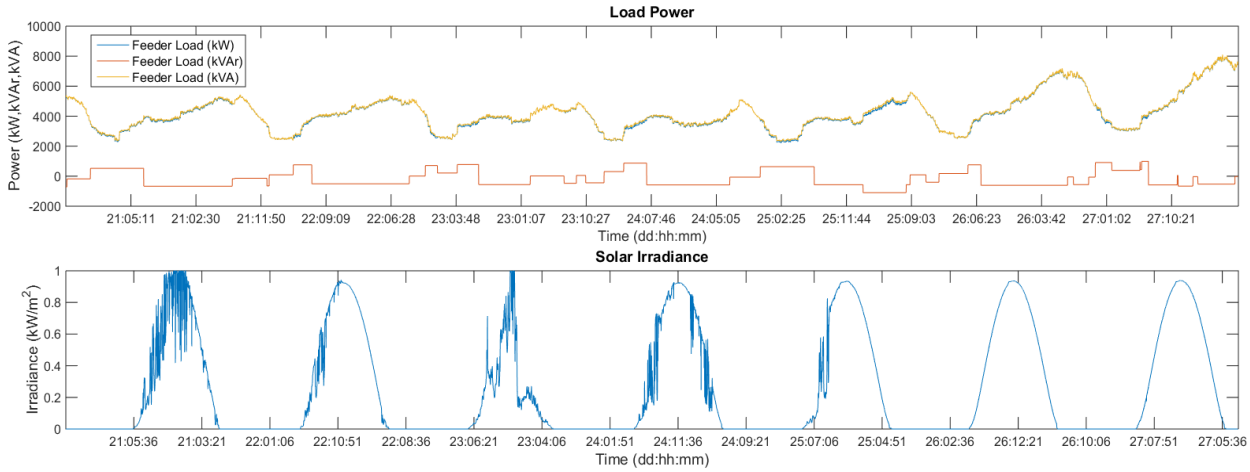

Figure 3. Weekly 1-minute resolution load and irradiance data selected for QSTS simulation to be representative of year.

The left plot of Figure 4 below shows how the voltage of a bus near the end of the feeder fluctuates due to the load profile from Figure 3. It even violates the ANSI low-voltage limit for several hours in the last two days. In the right-hand plot, a 1MW PV system with no advanced inverter controls has been added to follow the irradiance data from Figure 3. The voltage has much greater variability and violates the ANSI high-voltage limit many times. The goal of this research is to apply a control to the inverter of this PV system to mitigate these adverse voltages.

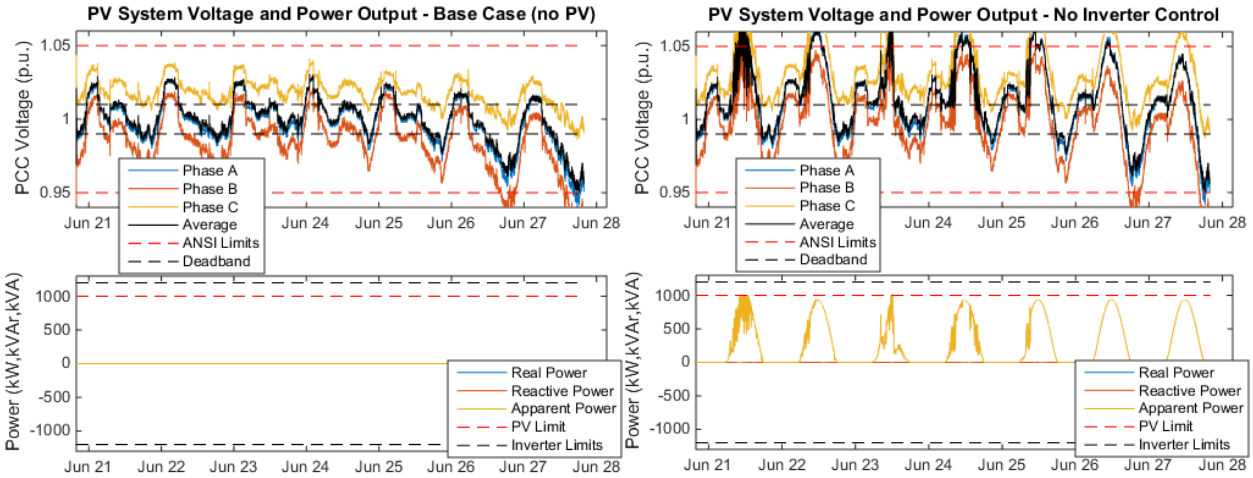

Figure 4. (left) Weekly simulation of end-of-feeder bus voltage and PV generation in the case of no PV and (right) with 1MW PV.

2.2.2. Ramp-Rate Control Example

The first control type is simply limiting the up-ramp of the PV system's real-power output to smooth out larger variability. The application of this control is shown below in Figure 5. In the left plot we can see the PV system is outputting less power on the cloudy days with large irradiance variability. However, the power output is smoother which makes the voltage less variable. The ramp-rate was set to limit the PV system to increase $0.4P_{pu}/h$, or $400kW/hr$ (40% of its 1MW rating). Zooming in on a period of high ramping in the right plot, we can see that this control is indeed limiting the power output increases by the correct amount. Another example is provided in Figure 6 at a ramp-rate limit of $0.1P_{pu}/h$, which shows the up-ramp of the PV limited to the correct amount of 100kW in a one-hour time period for the 1MW system. Here it is clearer that the down-ramp is not limited by this control, which physically makes sense. The fastest transients in the irradiance profile used will increase the output of the PV system by 0.5pu in one minute, or 30 P_{pu}/h. Any ramp-rate settings above this value would have no effect.

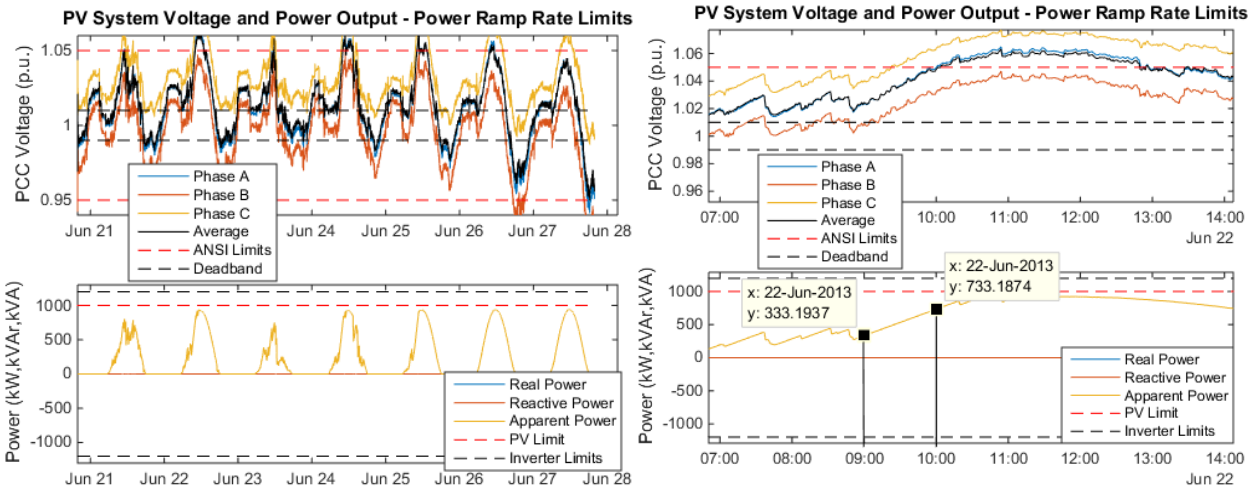

Figure 5.(left) Power ramp-rate limiting applied to the PV inverter. (right) A zoomed-in segment of time showing ramp limiting.

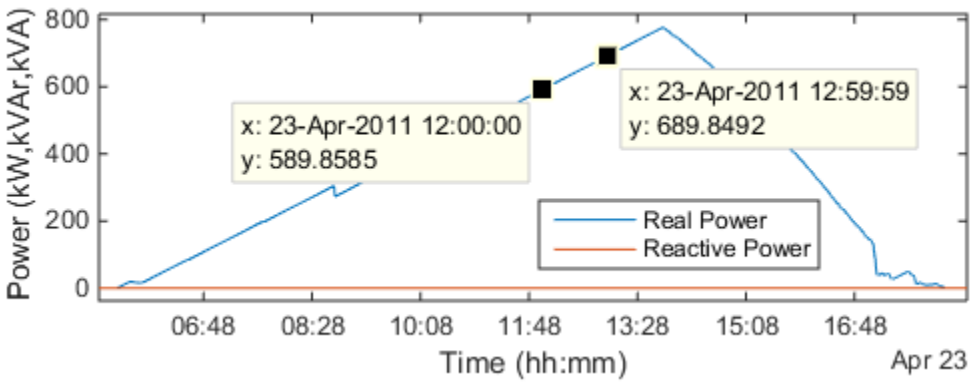

Figure 6. Single day of PV power output with a ramp-rate limit set to $0.1P_{pu}/h$.

2.2.3. Volt/Var Control Examples

The next two plots in Figure 7 demonstrate the two options for performing Volt/Var control. In the left plot, the control is limited by the real power output of the PV system, while in the right plot the real power output is curtailed to prioritize the reactive power control.

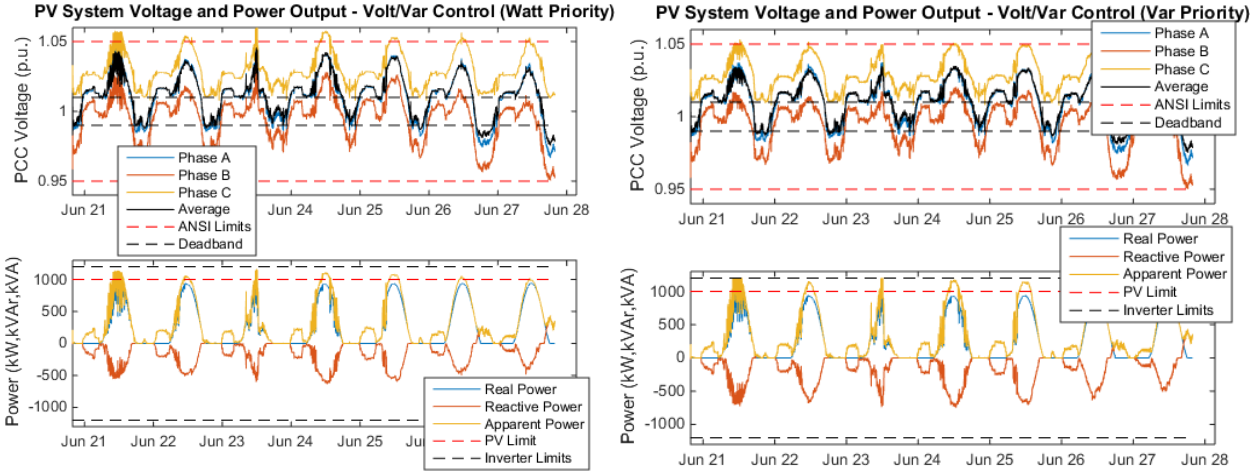

Figure 7. 1MW, 1.2MVA PV system with (left) Watt-priority Volt/Var control and (right) Var-priority Volt/Var control.

Although there is a clear difference between the reactive power generated between the two control versions, there is not a clear "prioritization" of reactive power in the Var-priority control evident by real power curtailment. To further demonstrate the functionality of the Var-priority control, since it was programmed in Matlab, a Volt/Var curve that attempts to regulate the voltage to 0.95p.u. is applied. This case is shown in Figure 8 below and it is clear now that the control saturates at the inverter limits and completely curtails the real power output in the times where it cannot achieve the desired 0.95p.u. voltage.

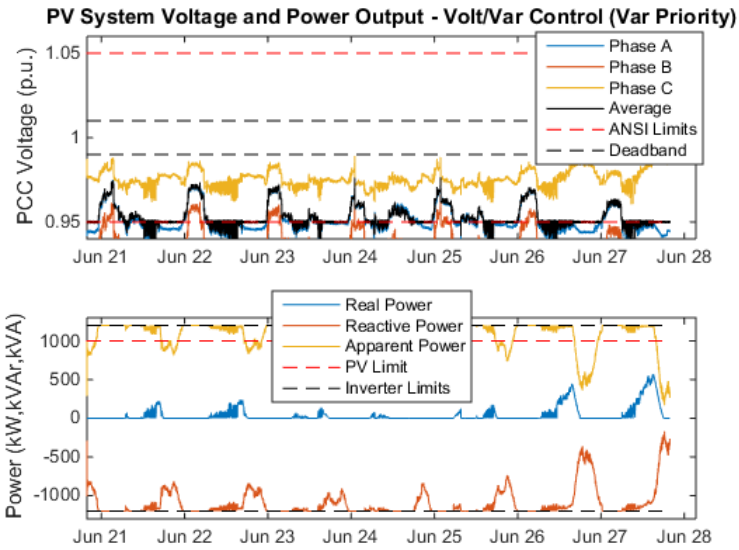

Figure 8. Var-priority Volt/Var control attempting to regulate average voltage to 0.95p.u.

2.2.4. Power Factor Control Examples

Figure 9, are shows the fixed and watt-triggered power factor controls. The fixed power factor control is set at 0.95 lagging and the watt-triggered power factor ranges from 0.98 lagging at zero PV output to 0.70 lagging at full PV output. It can be seen that the watt-triggered power factor produces more Vars, but is still ultimately limited by the rating of the inverter.

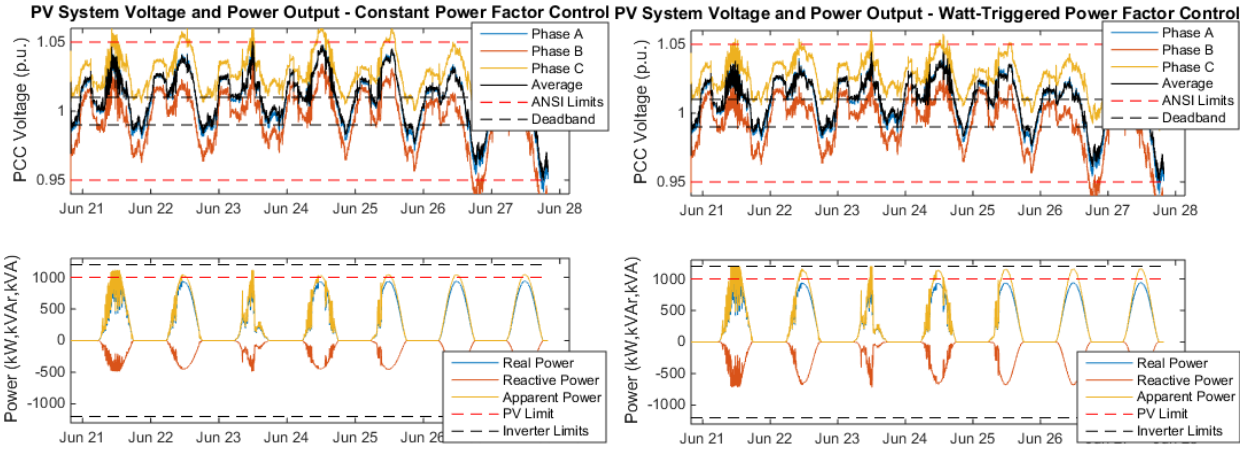

Figure 9. (left) Fixed power factor control at 0.95 lagging. (right) Watt-triggered power-factor control from 0.98-0.7 lagging.

2.2.5. Volt/Watt Control Examples

Lastly, Figure 10 shows the Volt/Watt control that curtails the real power output of the PV system based on the local measured voltage. In this instance, the curtailing only begins past the 1.05p.u. voltage violation. It can be seen that slightly less power is produced resulting in a slightly lower over-voltage between Figure 10 and the right-hand plot of Figure 4.

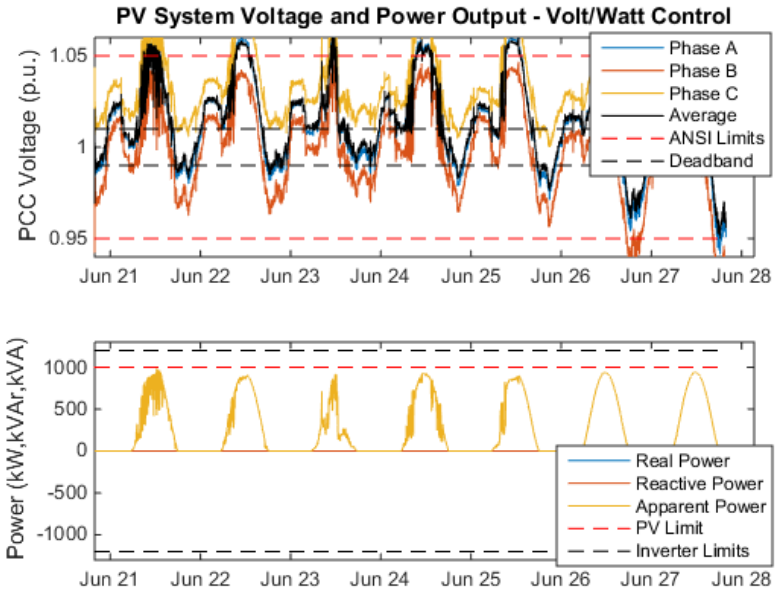

Figure 10. Volt/Watt PV curtailing control.

3. ANALYSIS METHODOLOGY

3.1. Study Feeders

Two distribution feeder models are used in this report to study the impact of the advanced inverter control types and their settings. The details of these two feeders are described below.

3.1.1. Feeder CO1

Feeder CO1 is a 12kV rural network with a peak load of 6.41MW. Its furthest bus is 21.4km from the substation. The feeder has one voltage regulator with a 15-second delay, 3 switching capacitors that switch on voltage, and two capacitors that switch on time. The location of these devices is shown in Figure 11 along with the voltage levels at peak load with no PV. The LDC fitting to find the most representative week of load for the year was presented in Figure 2 in Section 2.2. This resulted in the load and time-matched irradiance curves shown in Figure 3. The following results use this week of data in each QSTS study. Each control type described in Section 2.1 is tested at 20 PV locations using a 1MW PV system with a 1.1MVA inverter.

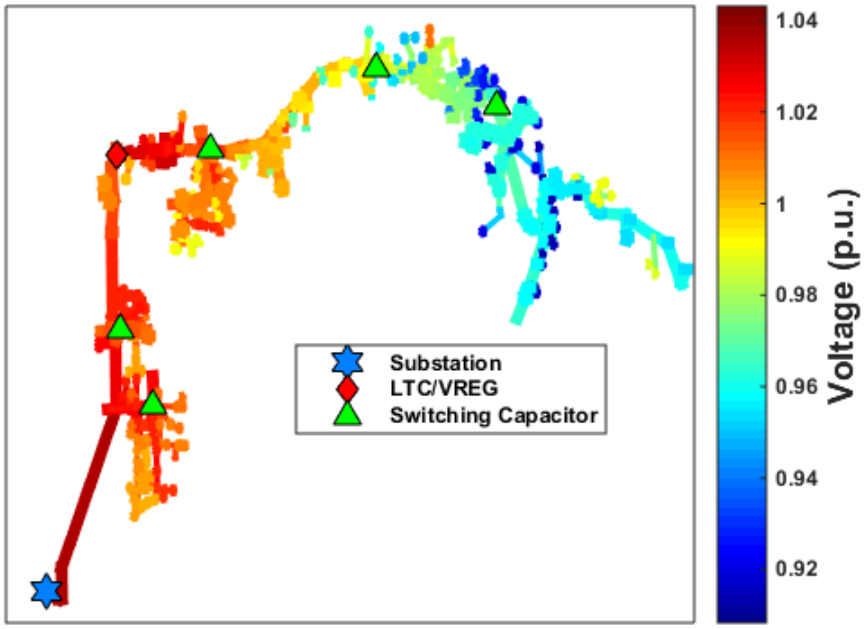

Figure 11. Feeder CO1 circuit topology with lines colored by voltage level at peak load.

3.1.2. Feeder CS1

Feeder CS1 is a 12kV agricultural feeder with a peak load of 9.23MW. The furthest bus is 11.9km from the substation. The feeder has two voltage regulators on 45-second delays and six switching capacitors that switch on either time, voltage, or temperature. The location of these devices is shown in Figure 12 along with the voltage levels at peak load with no PV. The LDC fitting to find the most representative week of load is presented in Figure 13. As before, the red line shows the LDC of the week of load that closest matches the LDC of the yearly load data,

represented by the black lines. To clarify, the dashed line is a one-week down-sample of the solid one-year line used to approximate what the desired week's LDC should look like. The load profile for Feeder CS1 does not have a continuous week that matches the year's LDC as well as Feeder CO1. The closest week of load that approximates the year's LDC is shown in the time domain in Figure 14. The same irradiance profile as Feeder CO1 is used on the PV system.

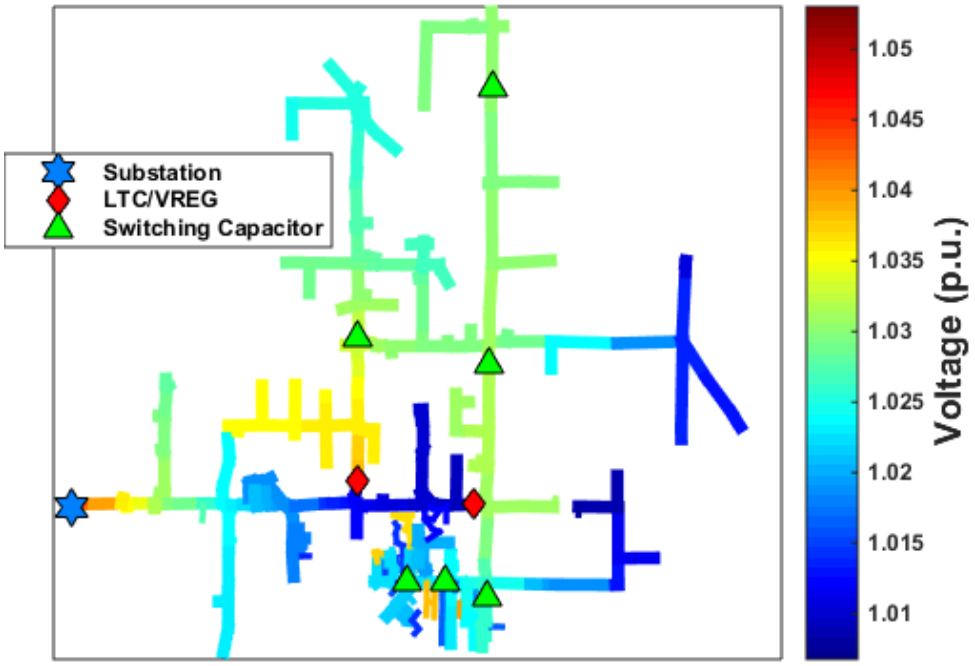

Figure 12. Feeder CS1 circuit topology with lines colored by baseline voltage level.

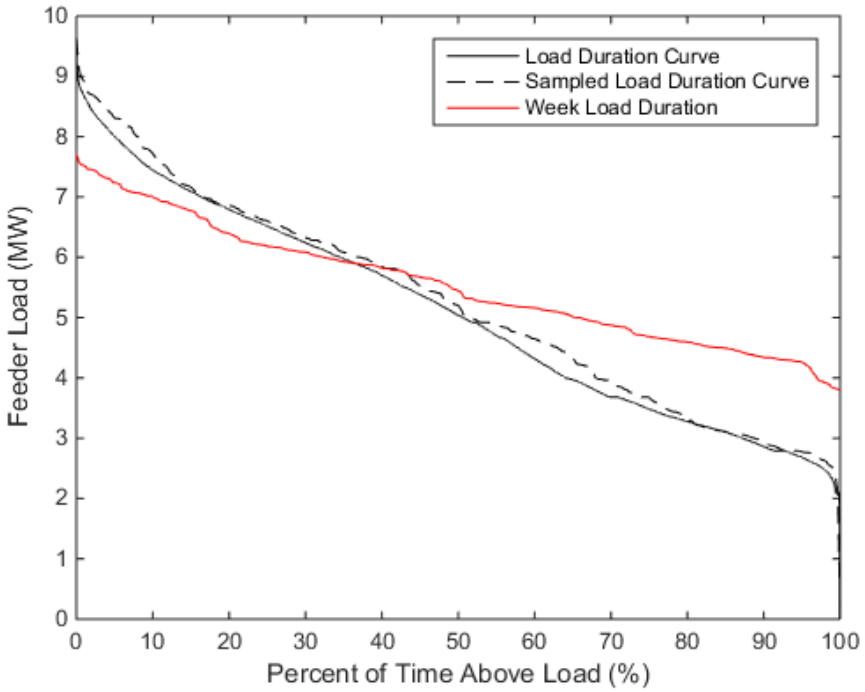

Figure 13. Week of load selected for the QS1 feeder by minimizing the error of its LDC to the year of load.

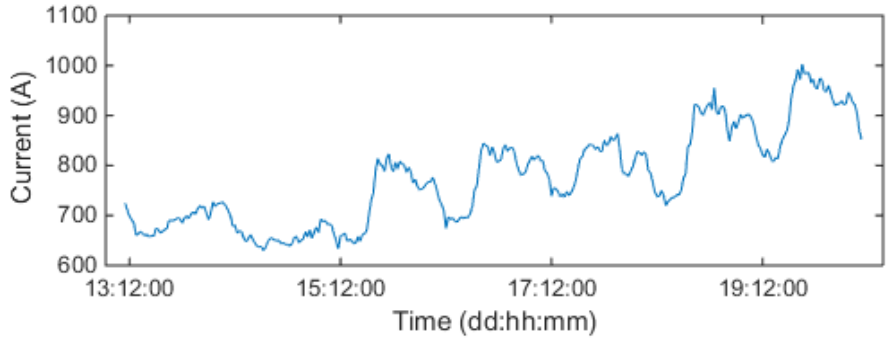

Figure 14. Load profile to be normalized and applied to each load in QS1 feeder.

3.2. Measured Impact of Inverter Controls on Network

3.2.1. Network Metrics Considered

Below is a list of each network measurement to be quantified over a time-series simulation that will gauge the success of each control described above at mitigating the negative impact of PV. Each metric is measured for the base case of PV at unity power factor and individually for each type of advanced inverter control.

- Time over-voltage (OT) – total simulation time during which any bus is over $1.05V_{pu}$.
- Time under-voltage (UT) – total simulation time during which any bus is under $0.95V_{pu}$.
- Regulator tap changes (TC) – sum of all voltage regulator tap changes that occur during the simulation.
- Capacitor switches (CS) – sum of all capacitor bank switching operations that occur during the simulation.
- Network losses (L) – sum of all line and equipment losses incurred on the network during the simulation in kWh.
- PV power curtailed (PC) – total PV power curtailed by the control during the simulation.
- PV vars generated (VG) – total reactive power generated by the PV inverter due to the advanced inverter control during the simulation, which may incur a cost to the customer.

3.2.2. Performance of Controls with Generic Parameters

Using parameters in the middle of the ranges defined in Section 2.1, each control is simulated on a 1MW PV system with a 10% overrated inverter at ten separate locations on a test circuit. The purpose of this test is to get a sense of how the performance of the controls varies with respect to the PV interconnection location. If there is little or no locational dependence in the circuit then it will not be necessary to test many PV interconnection locations. The percent changes in each network metric due to each control at ten locations are summarized in Figure 15 through Figure 20.

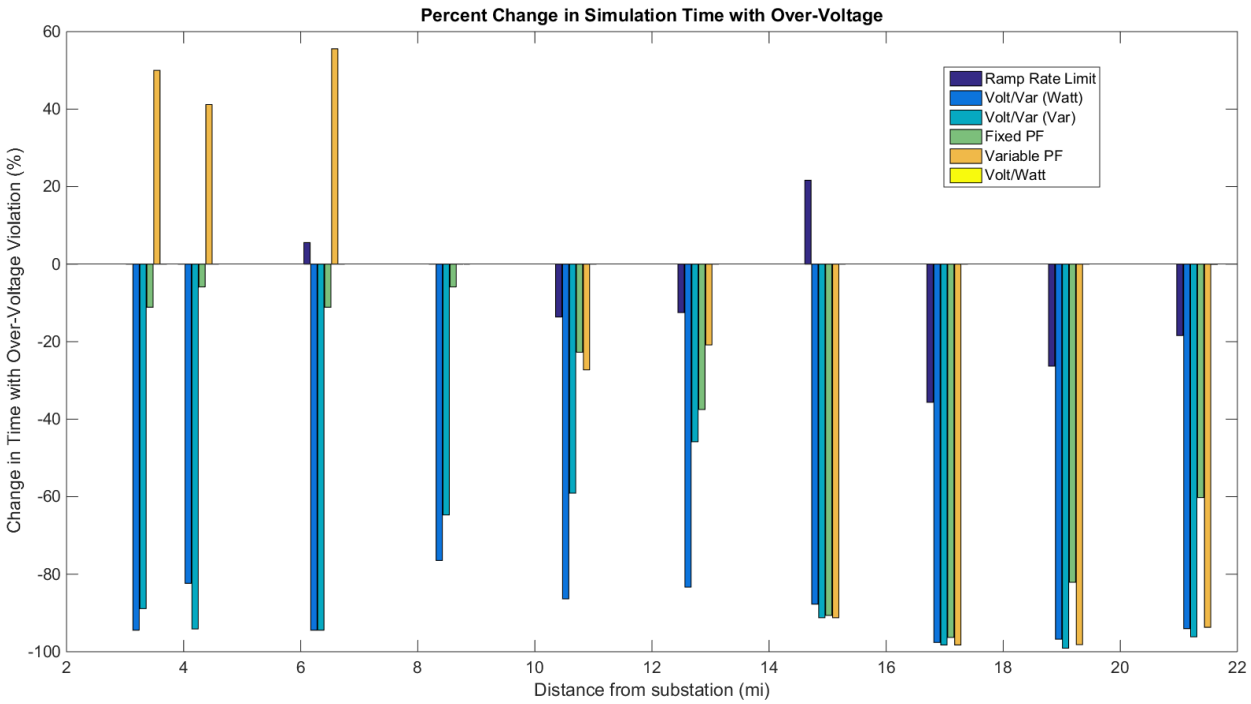

Figure 15. Percent change from no-control case in total simulation time with an over-voltage violation at several PV placement locations.

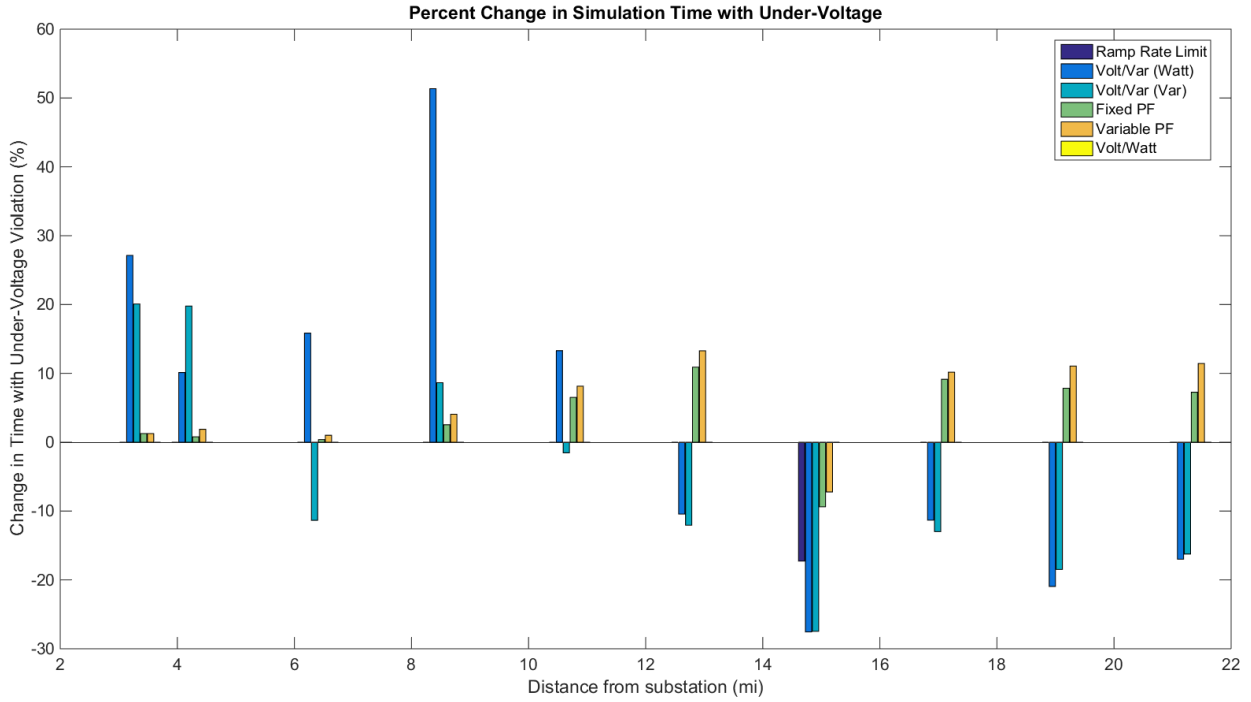

Figure 16. Percent change from no-control case in total simulation time with an under-voltage violation at several PV placement locations.

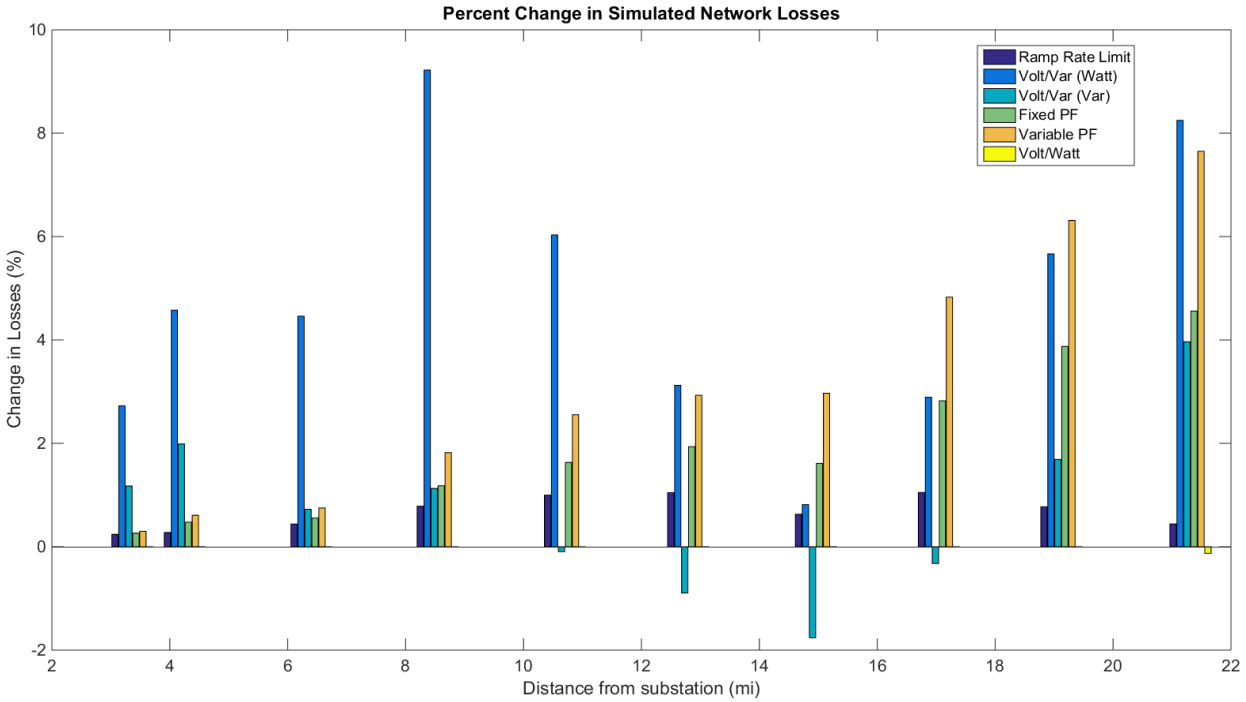

Figure 17. Percent change from no-control case in network losses at several PV placement locations.

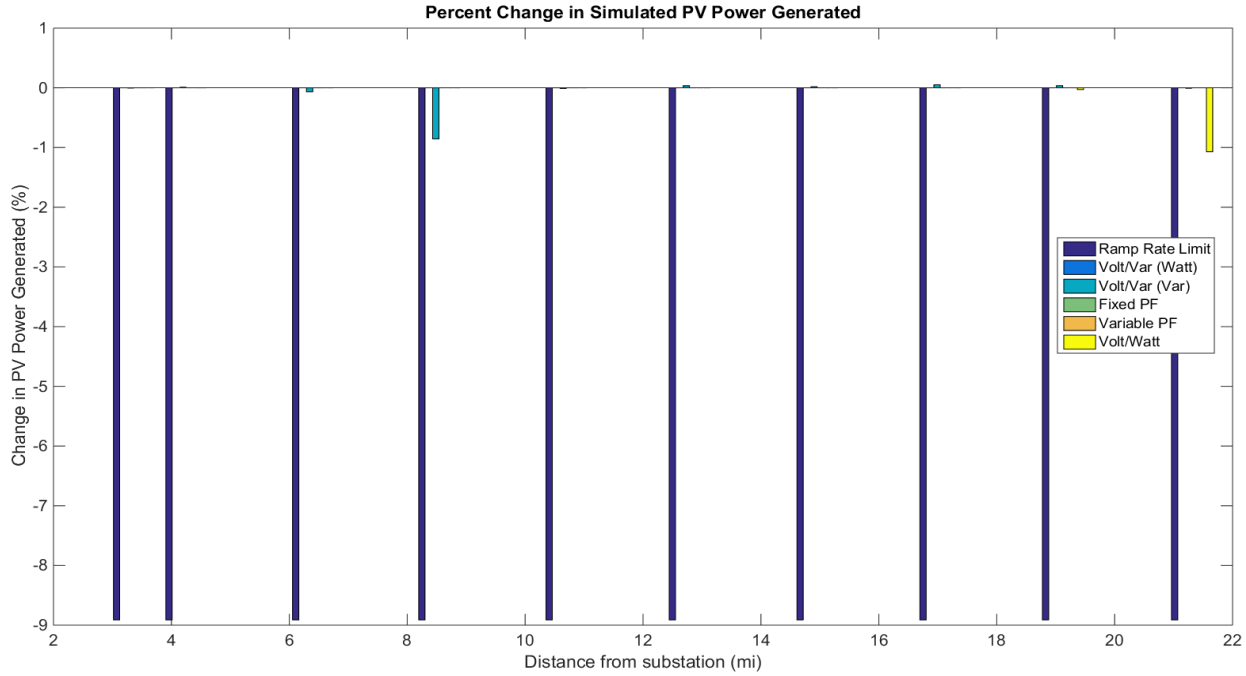

Figure 18. Percent change from no-control case in PV power generated at several PV placement locations.

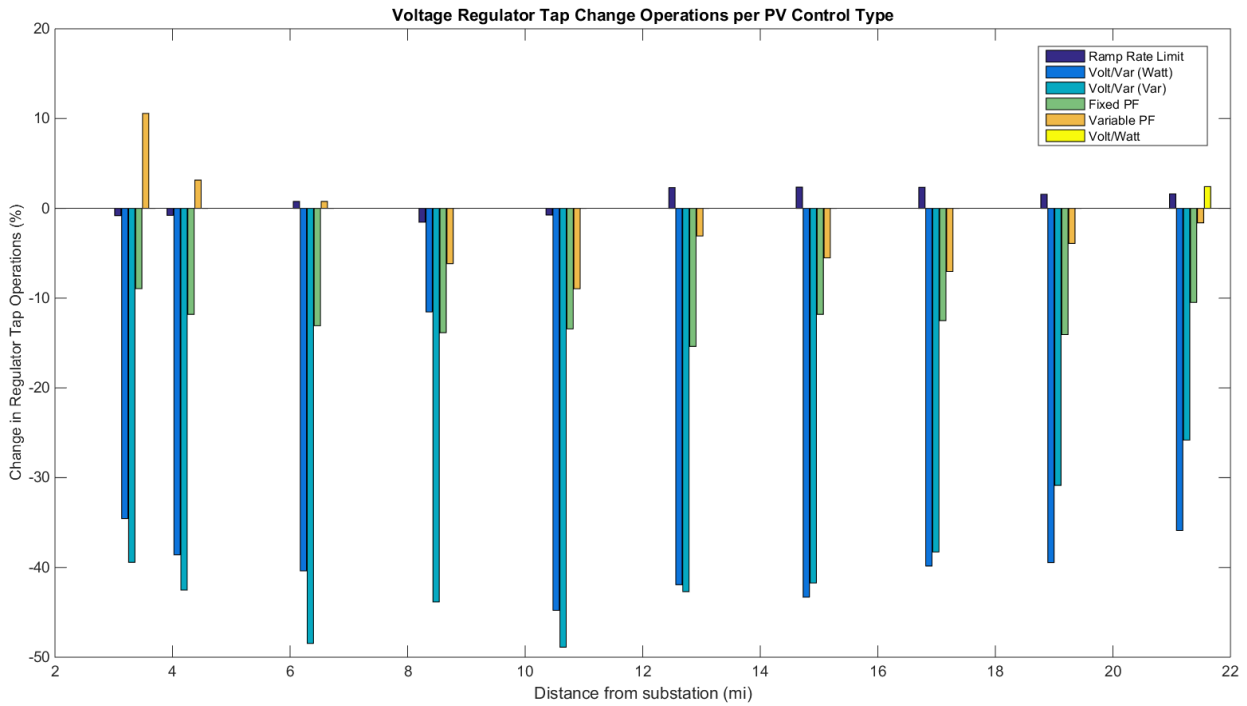

Figure 19. Percent change from no-control case in total number of tap changes during simulation at several PV placement locations.

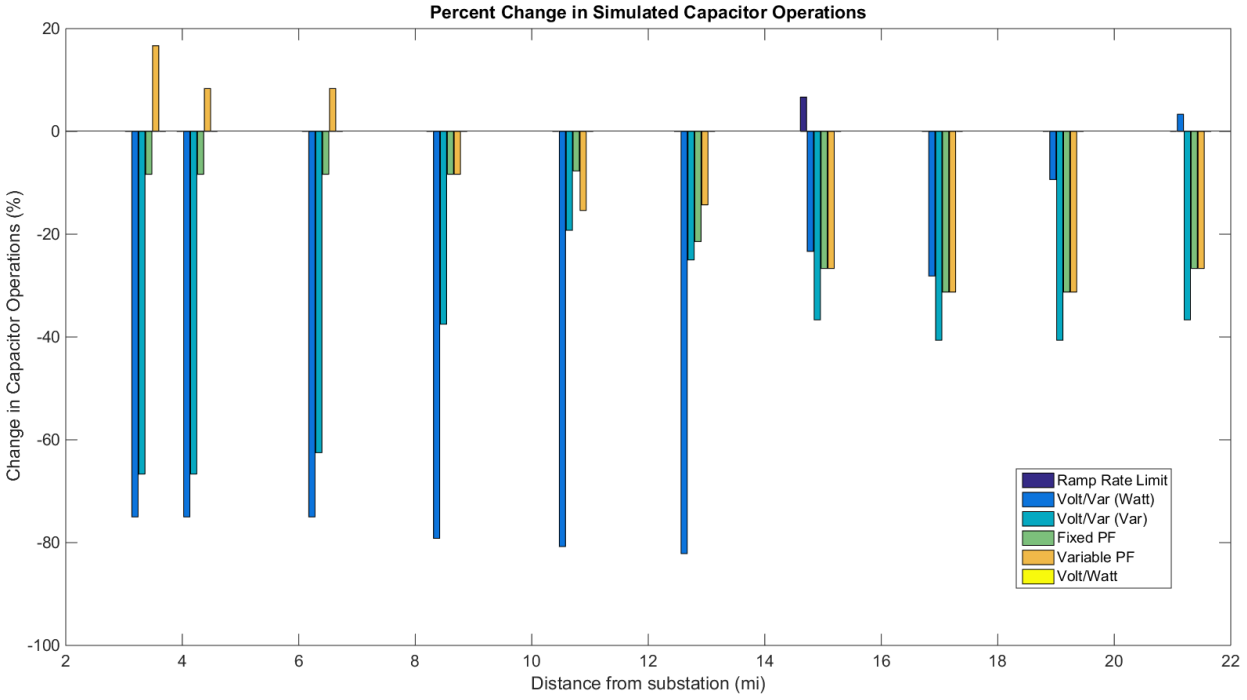

Figure 20. Percent change from no-control case in total number of capacitor switches during simulation at several PV placement locations.

As can be seen in Figures 15-20, the controls in general benefit the network metrics. There are, however, a few instances where the control actually degrades the performance of a metric. In particular, the watt-triggered power factor (listed as "variable PF" in the plots) control has a

tendency to make all metrics worse when it is used close to the substation in this feeder. Also, just about every control type tends to increase the losses compared with the no-control case, as seen in Figure 17. This makes sense since either the curtailment of local generation or the injection of vars is increasing the total line current as compared with the no-control case, thus increasing losses. Another particularly poor performance is the ramp rate limit's curtailment of PV generation compared with the other controls. This also makes sense because a more limiting ramp-rate limit of $0.5\,P_{pu}/h$ was used. However, ramp-rate limiting will still represent the largest PV curtailment, since it will decrease the amount of power generated for every steep increase in irradiance, regardless of the presence of adverse network conditions. Also, Figure 16 shows that most controls do not reduce the occurrence of under-voltage violations very well if not tuned well. The most important trend to point out, however, which is present in each plot, is that there is indeed a correlation between the effectiveness of an advanced inverter control and the PV location in the feeder. How performance changes for different controller parameters is investigated in Figure 21. Here, each unique color at each PV placement location represents a unique combination of the three control parameters used to tune watt-priority volt/var control. Any point in a positive value represents a net decrease in that metric's performance and a negative value represents a net improvement, except for the change in PV generation (which is negligible in this case). Although no specific setting suggestions can be gleaned from this plot, it does show that some parameter combinations are best used in some locations rather than others. In fact, there are several locations where it can be seen certain parameter sets increase the negative impact of the PV on the network rather than mitigate it. However, it does not seem parameters are universally good or bad across the network. In particular, the parameters corresponding to the light blue points perform poorly at most locations, yet at some locations these parameters result in improvements.

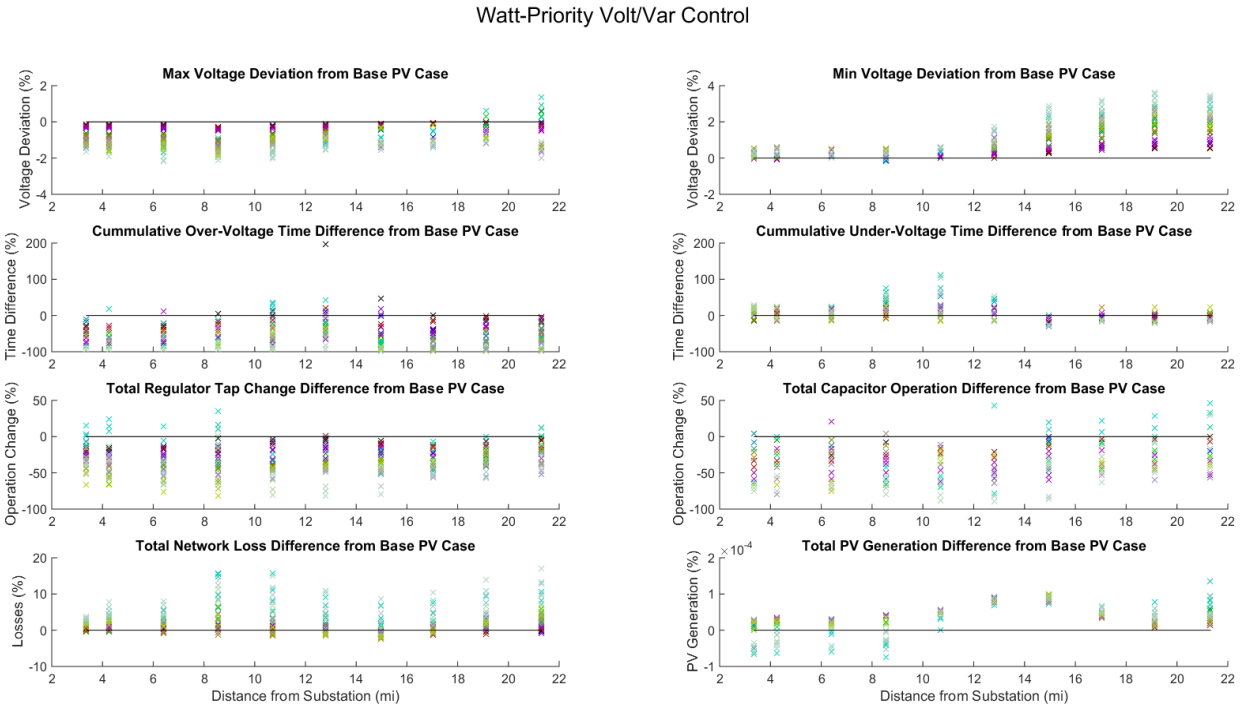

Figure 21. Impact of Watt-Priority Volt/Var control parameters on network metrics. Each colored point represents a unique combination of control parameters at each interconnection location.

3.3. Scoring Positive or Negative Controller Impacts

The previous section concluded that controller parameters cannot be universally deemed good or bad for improving a PV's impact on a distribution network. This section describes the method by which the metrics resulting from advanced inverter controls are deemed positive or negative overall. Each vector of metrics, $\boldsymbol{m}$, refers to the network metrics described in Section 3.2.1. The procedure is described in the following steps for any given control type:

1. Solve base case QSTS with no PV, record base metrics, $\boldsymbol{m_b}$
2. Place PV at interconnection location
3. Solve QSTS with no PV control, record metrics, $\boldsymbol{m_{nc}}$
4. Set inverter controller with parameter combination i
5. Solve QSTS with PV control, record metrics, $\boldsymbol{m_i}$
6. Find difference in metrics solely due to controls: $\Delta\boldsymbol{m_i} = (\boldsymbol{m_i} - \boldsymbol{m_b}) - (\boldsymbol{m_{nc}} - \boldsymbol{m_b})$
7. Apply relative importance weight to metrics: $\Delta\boldsymbol{m_i^w} = \boldsymbol{w} \cdot \Delta\boldsymbol{m_i}$
8. Repeat steps 4-7 for all parameter combinations
9. Repeat whole procedure for all interconnection locations

Due to the formulation in Step 6 above, if a particular set of parameters has improved a particular metric, its value will be negative. That is to say the no-control case will have resulted in more negative impact metrics relative to the base case than the control case, or the control has improved the impact of the PV. Thus, once all control parameters are tested at a location, the ideal range of parameters can be identified by finding the largest continuous range of parameters that result in $\Delta\boldsymbol{m_i^w} < \boldsymbol{0}$. The procedure for finding this range is covered in Section 3.3. In this research, the weighted change in metrics is defined below in (1) based on the metrics and symbols defined in Section 3.2.1.

$$\Delta\boldsymbol{m_i^w} = w_1 * OT + w_2 * UT + w_3 * TC + w_4 * CS + w_5 * L - w_6 P_{PV} - w_7 Q_{PV} - b \qquad (1)$$

In (1), b is a scalar bias that may be changed between control types to achieve a desired level of network improvement. In this research, the vector of weights used is $\boldsymbol{w} = [\,2\ 2\ 3\ 3\ 0.1\ 3\ 0.1]$. These weights indicate the relative importance of each metric, which are described in Section 3.1.1. Therefore, with this weighting the equipment operations are the most important network metrics and real power curtailment is the most important control cost. This weighting is necessary since slight improvements in voltage deviations and losses should not be scored as positive improvements if there is an increase in equipment operations. Here, the majority of metrics need to be improved for the control to be deemed successful. The PV power curtailed and vars generated are not included here because they directly contradict the $\Delta\boldsymbol{m_i^w} < \boldsymbol{0}$ threshold. Instead, once parameter ranges that lead to net improvements are identified, the absolute value of $\Delta\boldsymbol{m_i^w}$ can be compared to $PC_i + VG_i$.

3.4. Approximations Made to Reduce Computation Time

The ideal parameter identification procedure laid out in Section 3.2 is an exhaustive search of the parameter space for each control type. An exhaustive search is necessary due to the discrete,

discontinuous, and nonlinear nature of the solution space of $\Delta \boldsymbol{m}_i^{\boldsymbol{w}}$. However, this means as the dimensionality of the parameter space increases, the computation time increases geometrically. For example, if fixed power flow control is tested at a parameter granularity of 10, then only 10 QSTS simulations need to be performed for each PV interconnection location, in addition to the no-control case. However, for the two-parameter volt/watt control, 100 QSTS simulations need to be performed, and for the three-parameter watt-priority volt/var control, 1000 QSTS simulations need to be performed to span all unique parameter combinations. With such a large number of simulations necessary for even a decile level of parameter identification, certain approximations need to be made.

The first approximation has already been alluded to in Section 2.2: only one week of load and irradiance data is simulated in the QSTS rather than an entire year. A representative week of load is selected by minimizing the error between the yearly LDC of the feeder and the LDC of the week selected. A representative week of irradiance data is then matched to the week of load selected.

The second approximation is the time step size used in the QSTS. Figure 22 shows the percent change in the two most time-sensitive metrics, regulator tap changes and capacitor switches, due to various time step sizes. The highest resolution data available has a time step of one second and each increase from this changes the total number of tap changes and switches recorded. However, the change is still on the same order of magnitude between the time steps, meaning an approximation of how the network will change due to each control type can still be made.

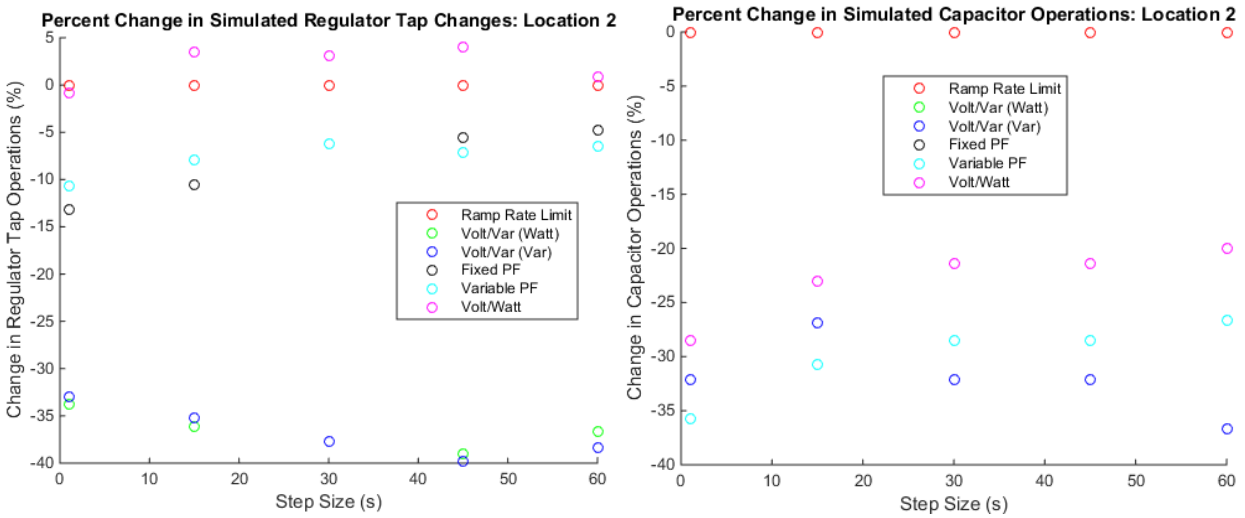

Figure 22. Percent difference in tap changes (left) and capacitor switches (right) using different simulation time steps under the various control types.

Furthermore, for similar results, the QSTS computation time required decreases exponentially for each increase in time step size. This trend is demonstrated in Figure 23. The worst-case scenario in this figure is the var-priority volt/var control, which must communicate over the COM interface between Matlab and OpenDSS several times each time step. This control takes over 10 minutes to calculate the one-week QSTS simulation at one-second time steps. At one-minute time steps, the one-week simulation takes less than 10 seconds. Therefore, in order, to simulate the large number of QSTS simulations required by an exhaustive search of the

parameter space (as previously described in this section) in any reasonable amount of time, a step size of one-minute is used in each QSTS simulation in this research.

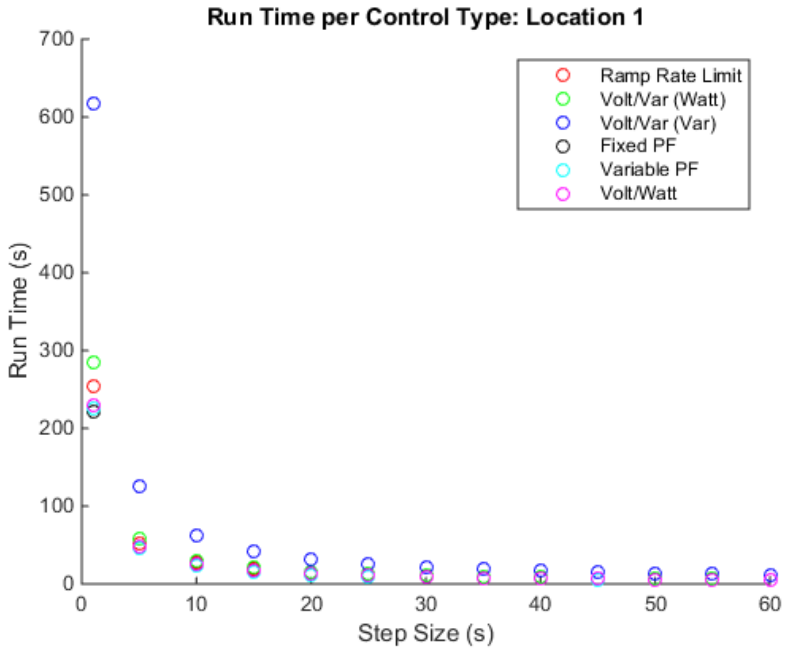

Figure 23. Computation time of each control type per data step size.

The third approximation is the use of reduced order network models. Extraneous elements such as short network branches, secondary networks, and clustered loads have been aggregated to provide a similar voltage profile on a much smaller network. The reduction process is described in [10].

3.5. Search Algorithm to Find Optimum Settings per PV Location

The algorithm to find the optimum range of control parameter settings depends on the number of parameters in the control. In the simplest case, for a single parameter, the region $\Delta \boldsymbol{m}_{\boldsymbol{i}}^{\boldsymbol{w}} < \mathbf{0}$ directly corresponds to an array of parameters. The "search" in this case simply verifies that all parameters that satisfy the $\Delta \boldsymbol{m}_{\boldsymbol{i}}^{\boldsymbol{w}} < \mathbf{0}$ requirement are continuous.

The problem becomes trickier in two or more parameter dimensions. Starting with two parameters and using volt/watt control as an example, the solution space of $\Delta \boldsymbol{m}_{\boldsymbol{i}}^{\boldsymbol{w}}$ can be visualized as a surface, as in Figure 24. It is clear now from this figure that the solution space is indeed nonlinear and discontinuous, making an analytical solution to the optimum parameter set difficult. The axes of this surface are the two parameters of volt/watt control: the slope of the PV curtailment due to PCC voltage and the deadband at which the control begins. The values in this space that correspond to the net score of the objective function and the control action. Net negative values represent control parameters that balance PV curtailment equally with an overall improvement of network parameters.

Only these negative values indicating good parameter combinations are shown in Figure 25. Now it becomes clear that finding a range of both parameters that encompasses the most improvement is not straightforward. The goal of finding the largest parameter ranges that only include good metric scores is equivalent to finding the largest rectangle that encompasses only colored blocks in Figure 25. To achieve this, an image processing tool called "FindLargestRectangle" is employed in Matlab. This function uses an optimization algorithm to maximize a rectangle in a Boolean bitmap image. In this case, the "image" used is the solution space from Figure 25, with negative values set to 1 and positive values set to 0. The largest rectangle, or largest intersecting range of acceptable control parameters, is highlighted over the entire surface in Figure 26.

This entire procedure is replicated for a PV interconnection placed midway down the feeder, and the results are shown in Figure 27. Comparing the two resultant rectangles, it can be seen that the PV interconnection location has a large impact on the range of viable control parameters. This result echoes the findings of Section 3.2 and means multiple PV interconnection locations should be tested to get a sense for the appropriate control parameters to use.

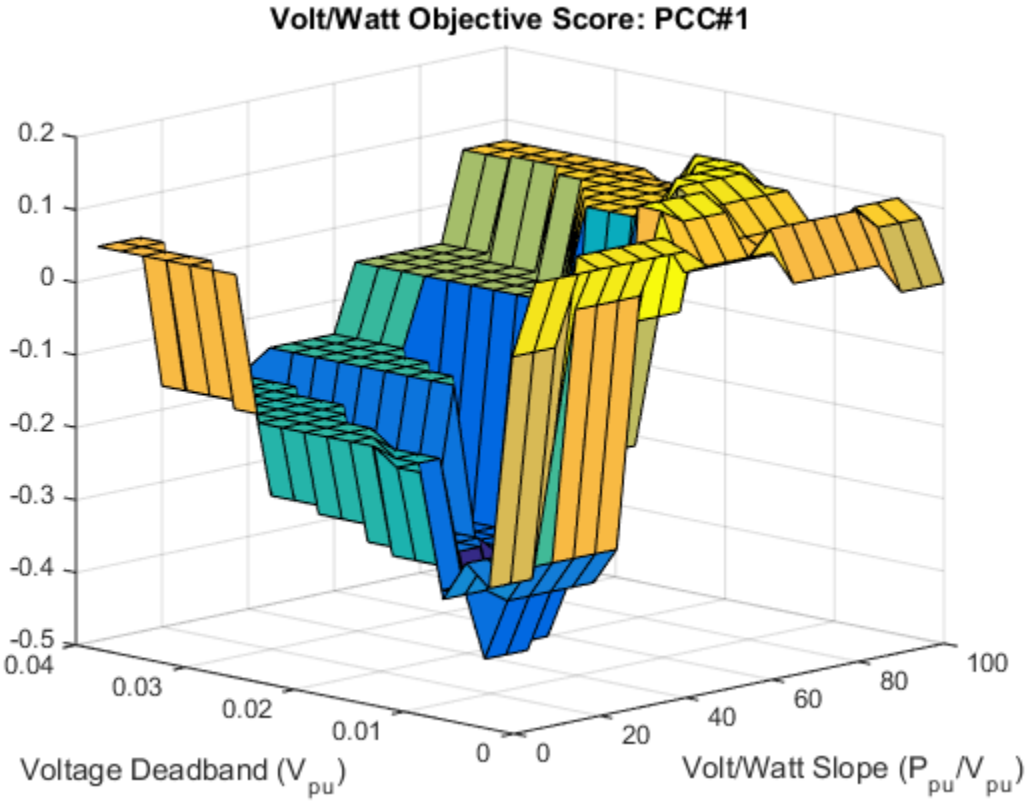

Figure 24. Solution space to the weighted objective function for volt/watt control at a given PCC.

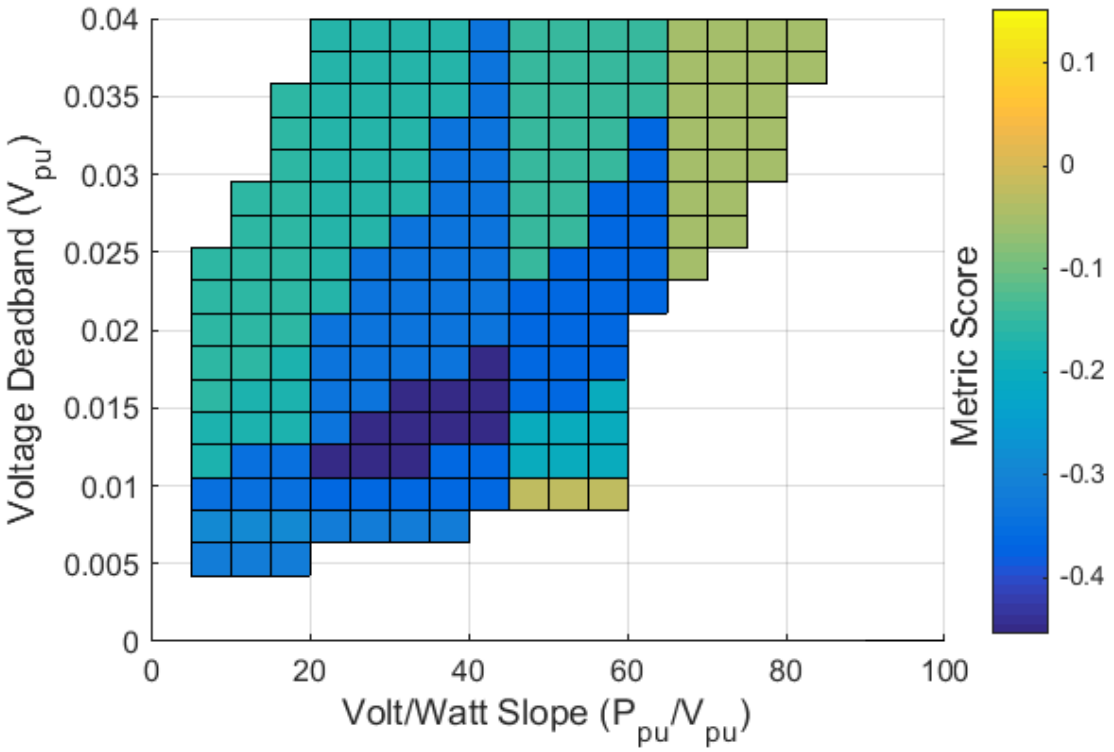

Figure 25. Volt/watt optimization solution space resulting in net-negative values.

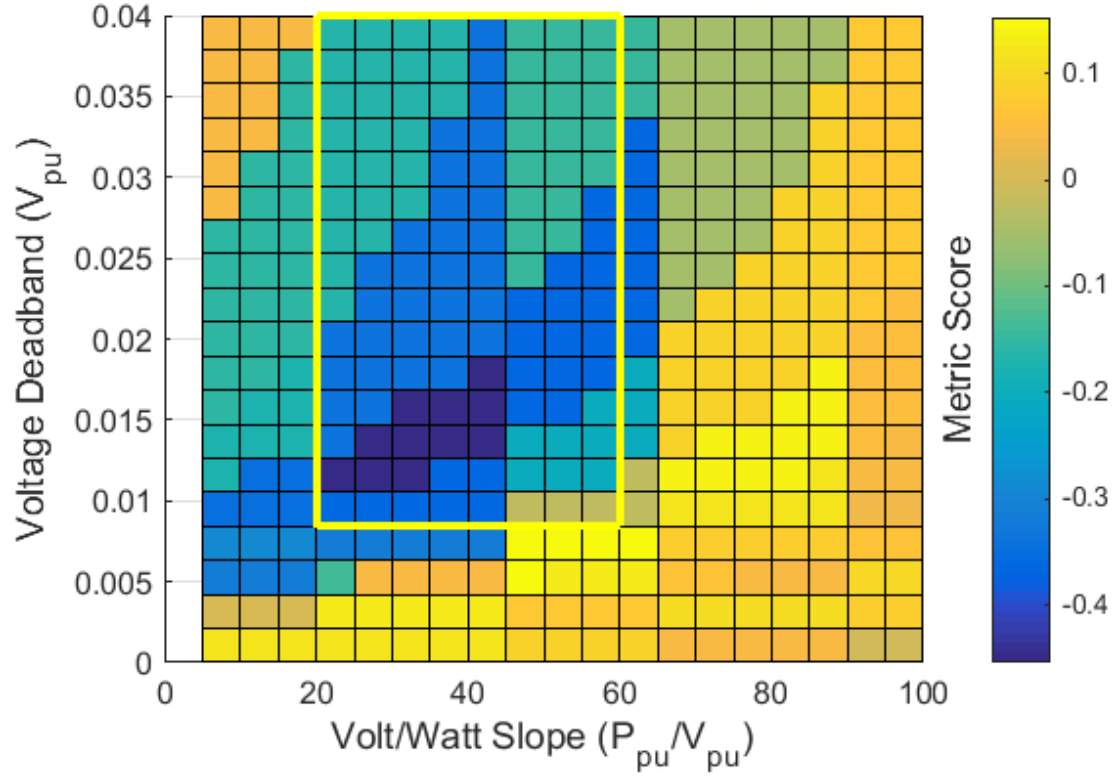

Figure 26. Largest range of parameters corresponding to net improvement due to Volt/Watt control at a PV interconnection at the end of the feeder.

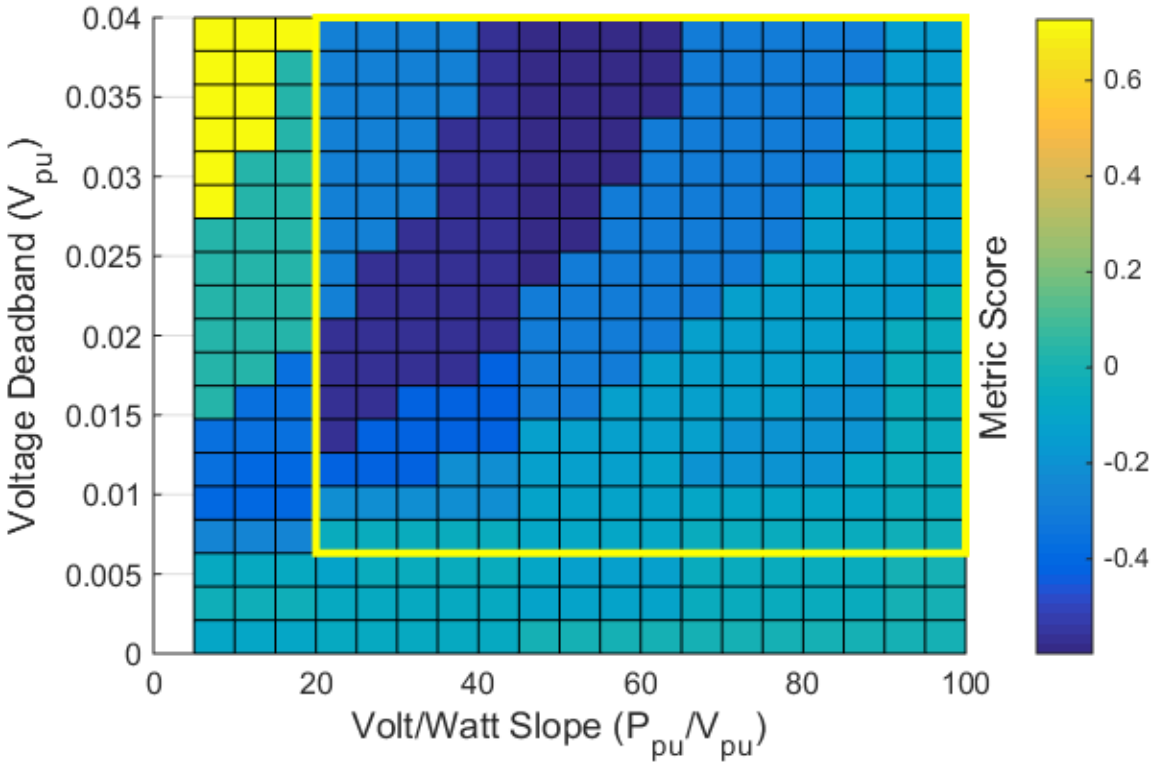

Figure 27. Largest range of parameters corresponding to net improvement due to Volt/Watt control at a PV interconnection midway down feeder.

To find the optimum range of parameters in the control types with three parameters (i.e. both volt/var controls), the methodology for the two-parameter case is applied to the two-dimensional solution space corresponding to each discretization of the third dimension. For any particular range of the third dimension parameter, the good values that span the entire third-dimension's range as well as the other two parameter dimensions are found by multiplying all the Boolean two-dimension solution spaces together. Then, the volume of the space that spans all three parameter dimensions is summed for every possible range in the third parameter dimension. The largest volume is kept and this represents the optimum set of parameters in all three parameter dimensions.

4. ADVANCED INVERTER CONTROL TYPE PERFORMANCE

This section will present the detailed results of each control type being run on one of the two feeders described in Section 3.1

4.1. Inverter Ramp-Rate Limiting

By simply limiting the rate at which the PV system is allowed to achieve a higher power output level, some of the adverse impacts on network metrics may be avoided at the expense of a slightly lower PV energy production. The impact on the various metrics and the amount of PV being curtailed at different rate limits is shown in Figure 28. Each of the colors represents one of the 20 different interconnection locations on feeder CO1. From the top plots, a general trend of improvement with increased ramp-rate limiting can be seen in tap changes on the left and capacitor switches on the right. However, only certain interconnection locations see improvements whereas several locations seem to gain improvement in these fields due to having PV regardless of its variability. The total amount of PV generation curtailed by each control type is shown in the bottom-right plot. The bottom-left plot shows the network losses, which generally increase with more curtailment since the PV is offsetting certain network current flows. Over-voltage violations, shown in the middle-left plot, generally decrease with more curtailment as expected. Under-voltage violations interestingly improve somewhat consistently when PV is placed at certain buses.

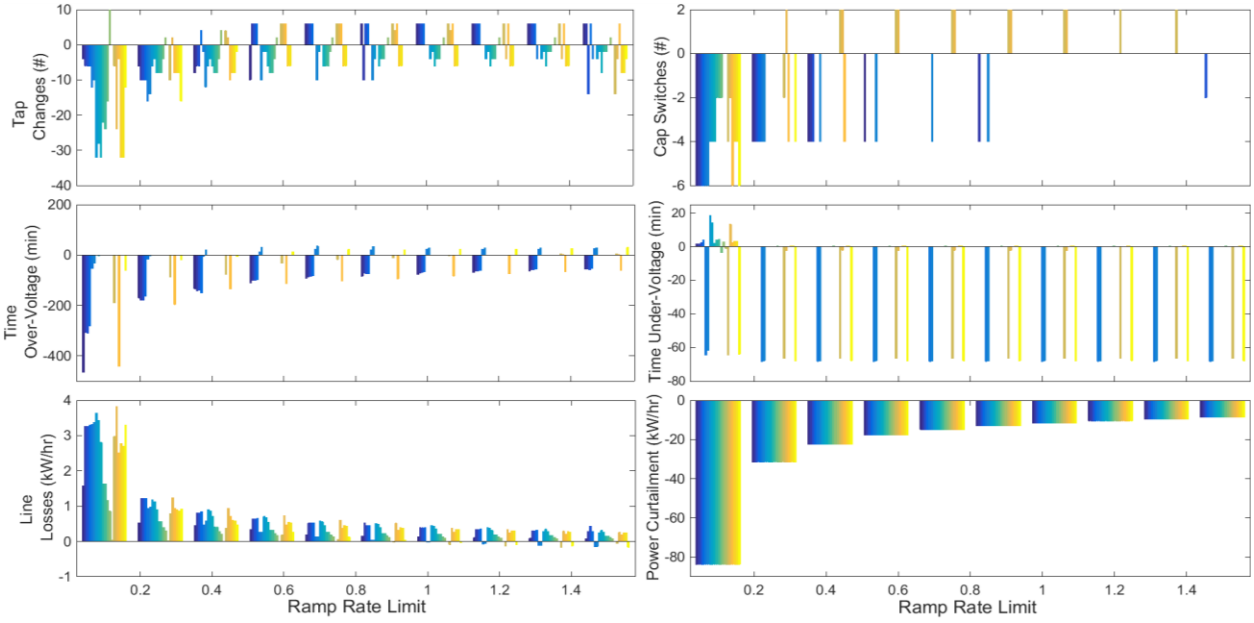

Figure 28. PV power curtailment and five network metrics as impacted by inverter ramp-rate limiting for 20 locations (different colors) on feeder CO1.

Due to the conflicting nature of some of the metrics shown in Figure 28, it is useful to get a sense of the overall improvement gained by the control at each location and setting. In Figure 29, each network metric (not including control action cost) is normalized to its minimum (best) value and summed together. The first thing to note in Figure 29 is that the positive green values are

indicative of that particular PV location showing no overall improvement for any of the control's parameter values. In other words, at this location the PV system always had a better impact on the network without ramp-rate limiting. The second thing to note is that there is a general trend of more overall improvement with increased curtailment. This is obvious since, unless the PV actually improved the system, the more PV is curtailed the closer the system returns to its baseline metrics. This is why a weighted objective score including the cost of the control is necessary. In Figure 30, the objective function in (1) is used to weigh control cost against network improvement. In this case, the settings that only slightly limit the ramp-rate of the PV perform slightly better than the other more aggressive control settings. This indicates that the improvements gained by limiting PV ramping are not significant compared with the cost of curtailment using these metric weights.

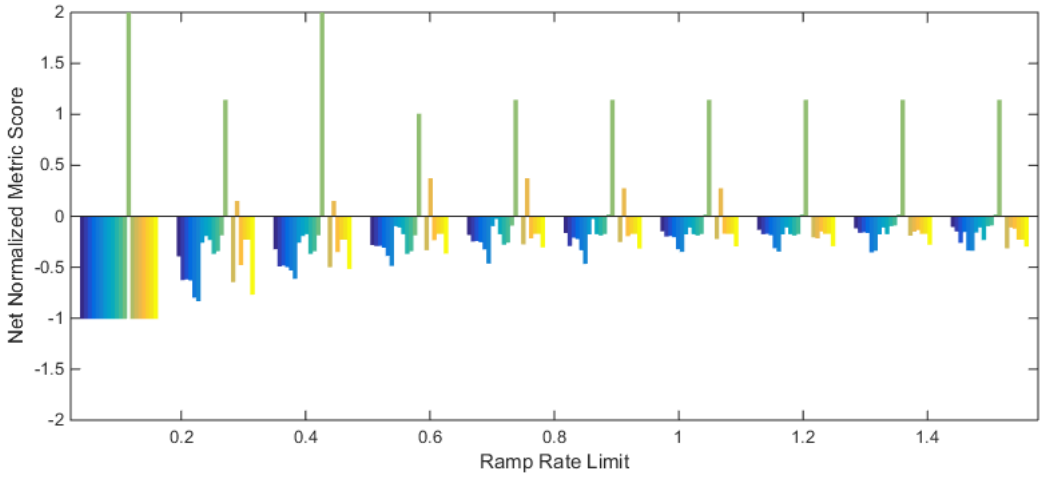

Figure 29. Sum of normalized metrics per ramp-rate limit.

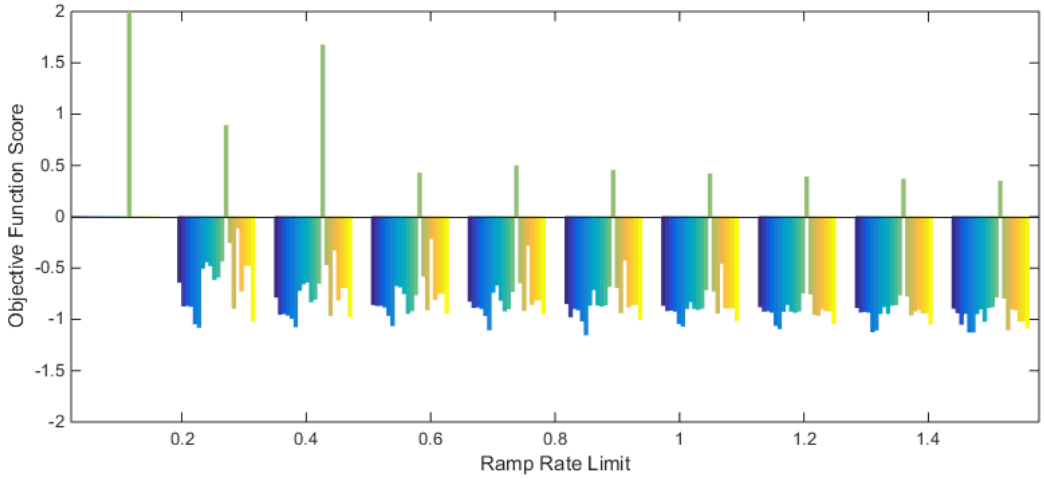

Figure 30. Weighted objective function (1) score per ramp-rate limit.

4.2. Constant Power Factor Control

With the inverter set to a constant power factor, the change in the base case of the five network metrics and the control action are shown in Figure 31. Each grouping of bars represents the net change from the no-control case for one particular control setting at all 20 interconnection locations in feeder CO1, where the locations are shown as different colors. Looking at the top-left plot, it can be seen that the reduction in tap changes peaks in general across the feeder at 0.9 power factor and at 0.8 power factor there are several interconnection locations that begin to see more tap changes due to the control. Capacitor switching displays a similar behavior in the top-right plot, except several of the power factors perform equivalently well. As expected, the number of over-voltages shown in the middle-left plot improves with increased reactive power absorption. However, this improvement plateaus around 0.85 power factor. Conversely, the number of under-voltage violations becomes worse as more vars are absorbed by the PV inverter, as shown in the middle-right plot. This is an indication of why an objective function is necessary to rate the control action, as some metrics may change in different directions. In the bottom-left plot, losses can be seen to increase in general as the inverter injects more reactive current into the network, which is to be expected. Lastly, the bottom-right plot shows the control action used by the inverter. In this case, it is the vars generated by the PV inverter, which of course increase with decreased power factor.

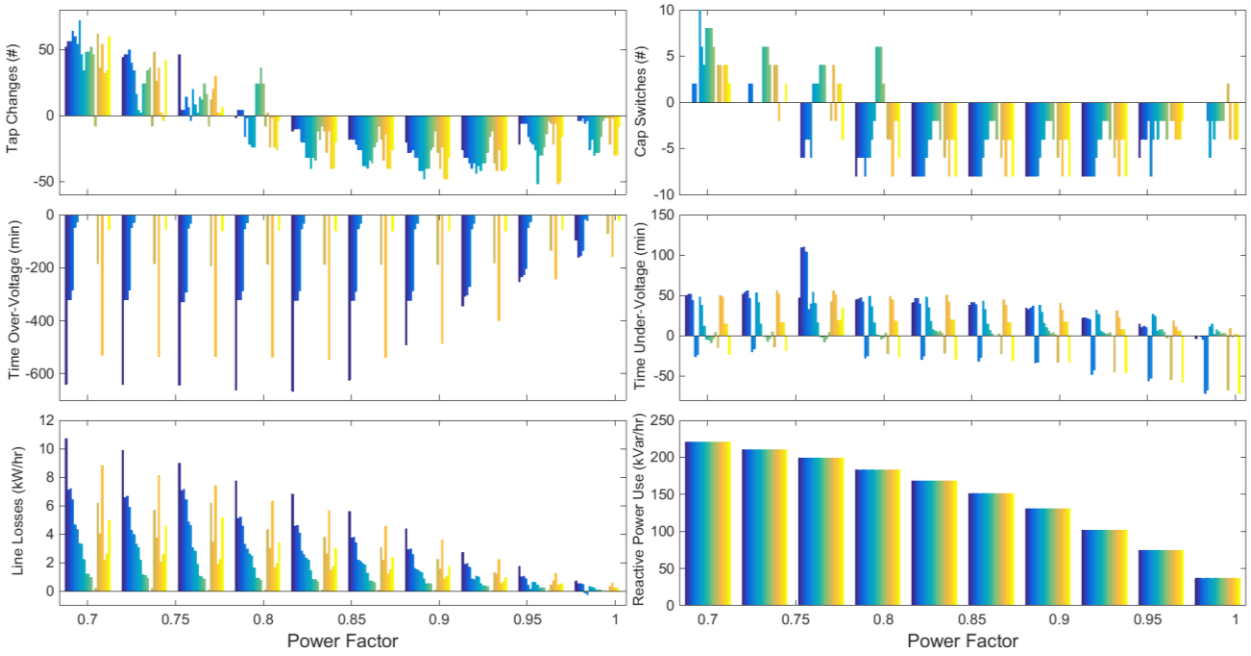

Figure 31. Inverter control action and five network metrics as impacted by inverter constant power factor settings and PV interconnection location on feeder CO1.

Again, due to the conflicting nature of some of the metrics, the sum of the normalized improvements is taken and displayed in Figure 32. Here it can be seen that across all locations a constant power factor between 0.9 and 0.95 shows the most overall improvement. This finding is echoed with the objective scores, which are displayed in Figure 33. The upper and lower boundaries that correspond to the widest range of good power factors settings at each location are shown per their interconnection location on the network maps in Figure 34.

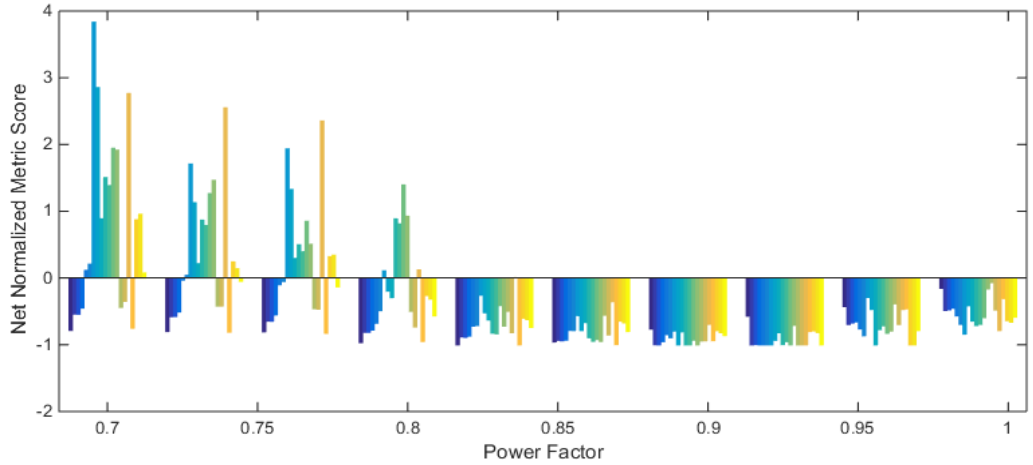

Figure 32. Sum of normalized metrics per inverter power factor.

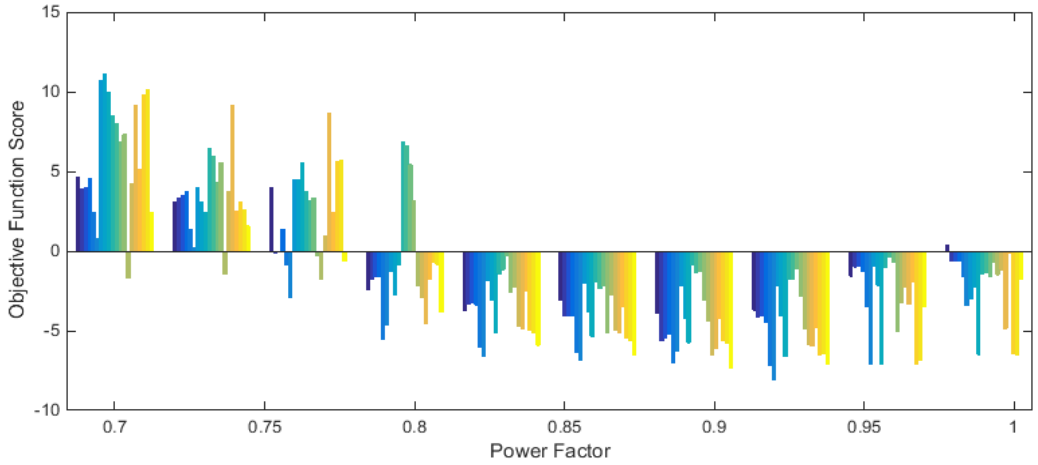

Figure 33. Weighted objective function (1) score per inverter power factor.

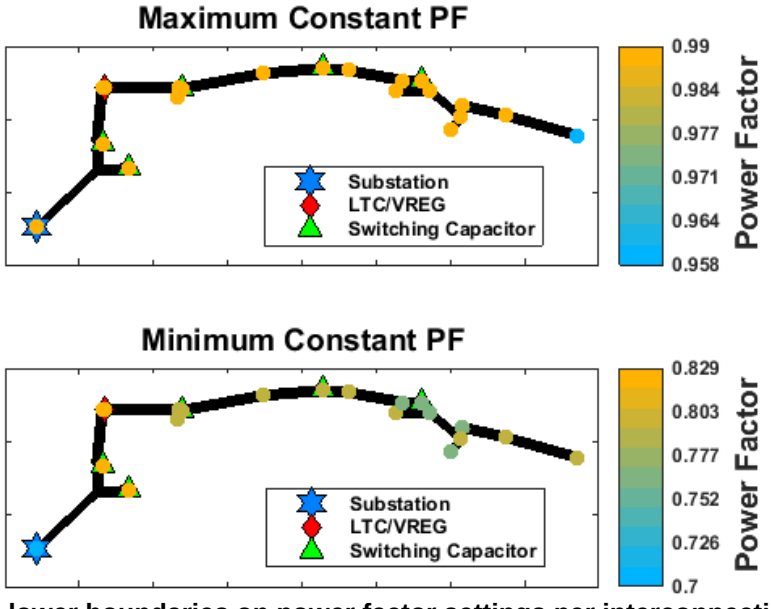

Figure 34. Upper and lower boundaries on power factor settings per interconnection location in feeder CO1 based on the metric weighting function (1).

4.3. Volt/Watt Control

For a two-parameter control, such as Volt/Watt, the network metrics become more difficult to visualize individually. The sum of the normalized network metrics for each unique combination of the two control parameters, at all interconnection locations, is presented in Figure 35. As with the ramp-rate limiting control before, there is a general trend of improving network conditions the more aggressive the controller curtails the PV. This is expected since more curtailment will mitigate any PV-induced issues. However, in this case the amount of improvement is more variable with PV location since the control relies on the local voltage, which have a strong or weak dependence on the PV output.

The objective function score (1) of each parameter pair at each PV location is presented in Figure 36. In this case, since the score of each control is now penalized for the amount of PV power curtailed, the most aggressive control parameters (high slope and low deadband) no longer register the minimum scores. It is clear that since there is almost a direct trade-off between the effectiveness of the control action and its cost that the best parameters to use should be somewhere in the middle of the ranges considered. However, the increased variability due to PV location makes it difficult to draw an overall conclusion.

Rearranging the data from Figure 36 to represent the control parameter surfaces such as the one in Figure 26, yields the set of twenty surfaces (one for each location) in Figure 37. Orange and yellow regions indicate a poor control response and green to blue regions indicate a good response. However, this continuous color scale applied across all locations makes it difficult to distinguish the boundary between good and bad parameter sets. Instead, a threshold can be chosen, as in Figure 25, under which there is an acceptable improvement in network conditions for the associated control cost. In Figure 39, a threshold of -1.0 is set and the yellow regions indicate the parameter sets that achieve at least this level of improvement against control cost. For most interconnection locations, there are a broad range of acceptable parameters. However, several regions have much narrower ranges. There is even an outlying location, represented in pale green, in which no set of parameters achieved an improvement below the given threshold. This is a location where Volt/Watt control of any kind would not be practical, indicating the presence of the PV may actually improve the overall network conditions when placed there.

The method described in Section 3.3 is then used to find the largest range of parameters that meet the minimum threshold requires of the objective function for each of the subplots in Figure 39. The upper and lower bounds of these areas are then plotted in Figure 40 and Figure 41 per PV interconnection location in feeder CO1. Figure 40 shows the minimum and maximum Volt/Watt slope settings that can be used at each PV location and still achieve the objective function goal. Figure 41 similarly shows the upper and lower Volt/Watt deadband settings to achieve this goal. As expected from the plots in Figure 39, many of the locations can be loosely set on the control parameters to achieve the desired goal. This of course depends on the weights given to the objective function (1) and the scalar bias. If, for instance, the weight of the PV curtailment control action is increased, then more aggressive control parameter sets will fall above the bias. Figure 40 indicates the upper bound of the controller slope is dependent on interconnection location, but not the lower bound. Similarly, the lower bound of the size of the deadband is location dependent, as seen in Figure 41.

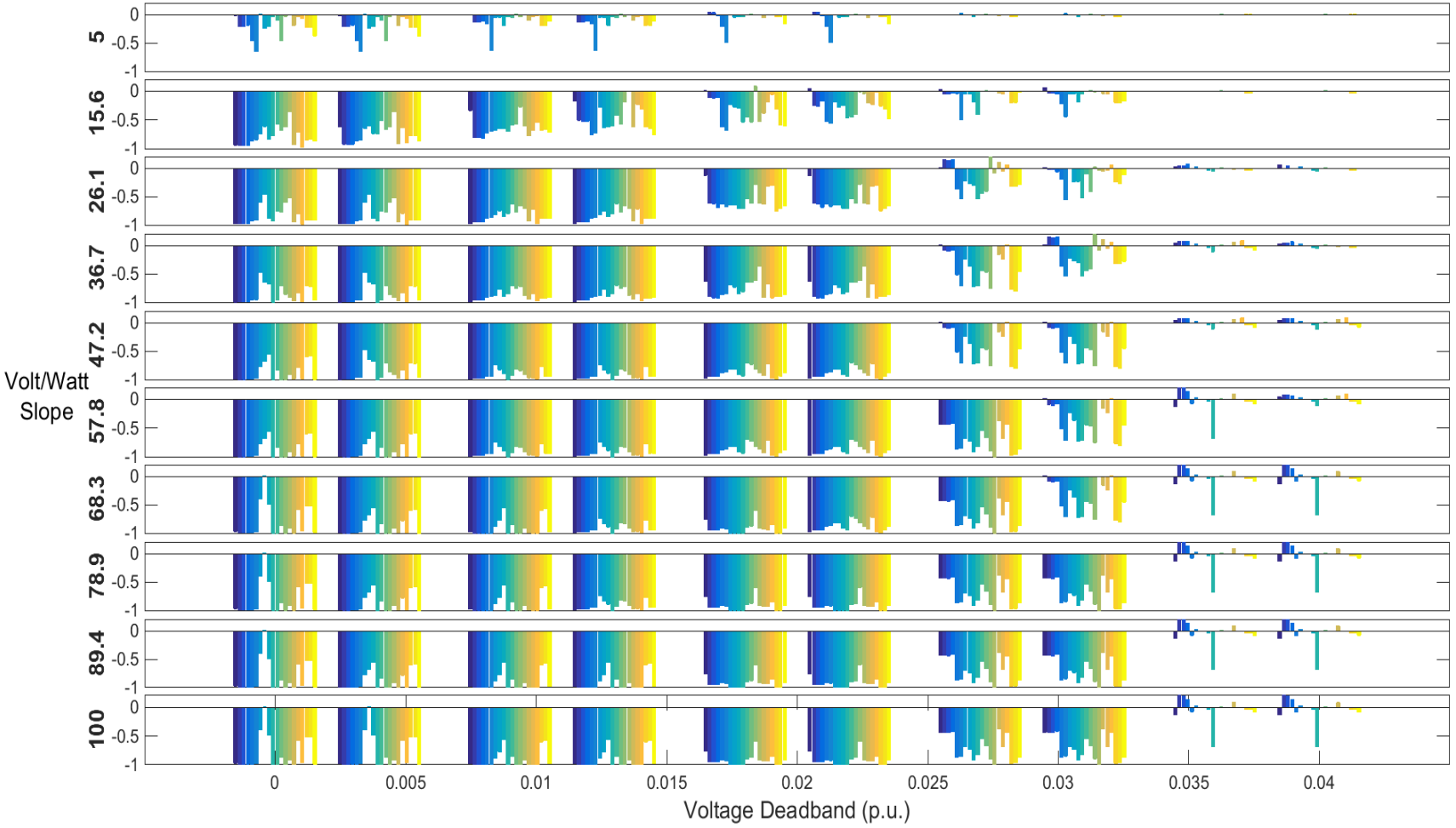

Figure 35. Sum of normalized network metric scores for each Volt/Watt control parameter at all PV locations.

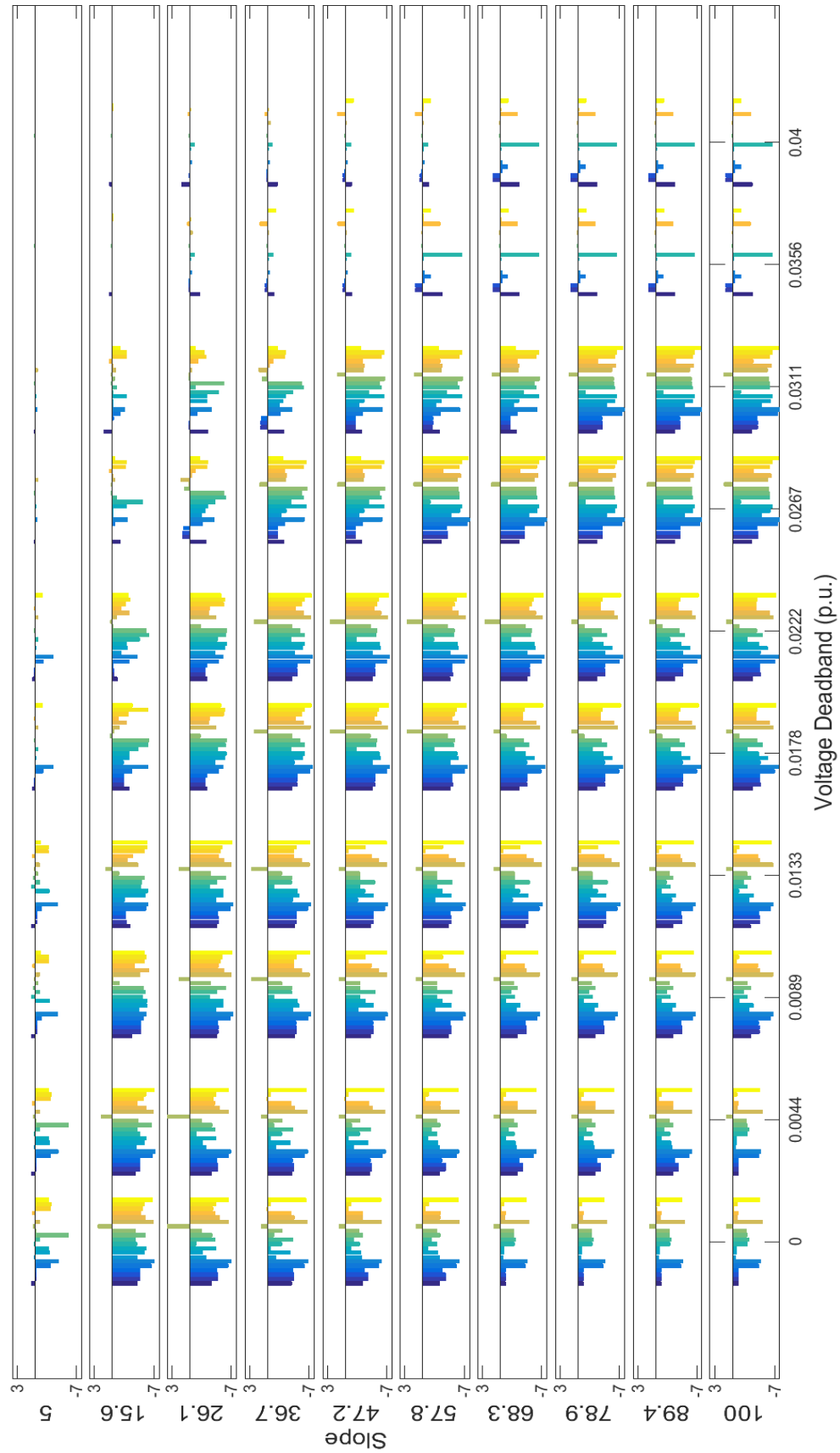

Figure 36. Objective function score for each set of Volt/Watt control parameters at all PV locations.

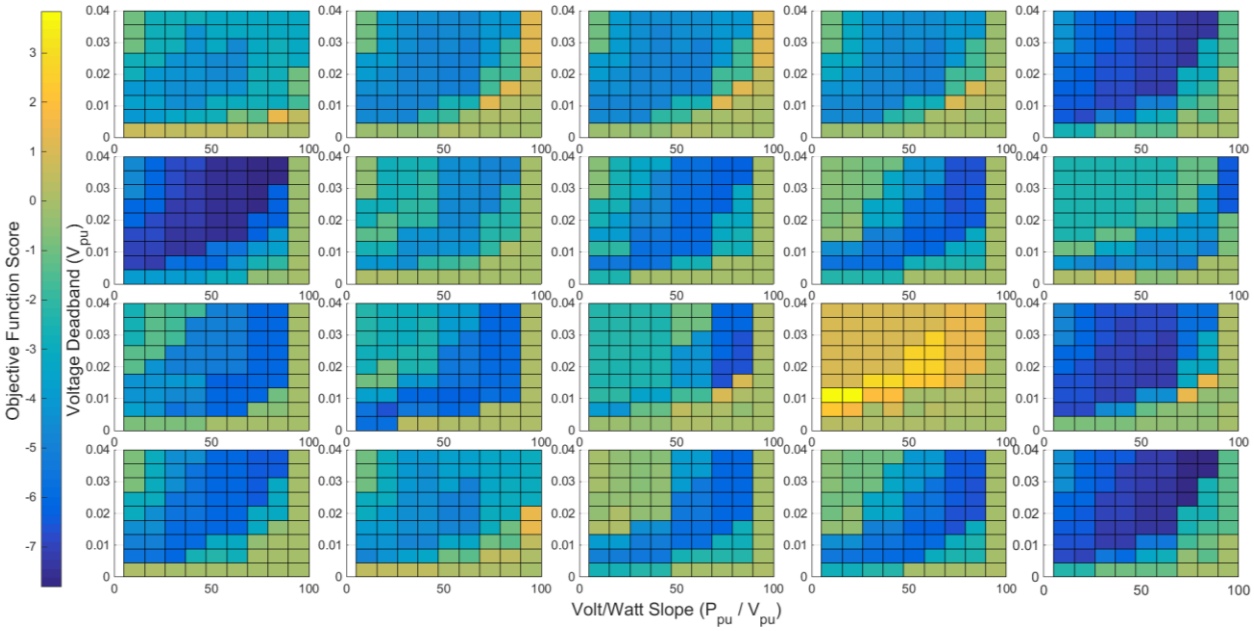

Figure 37. Volt/Watt control objective function score surfaces at each PV location.

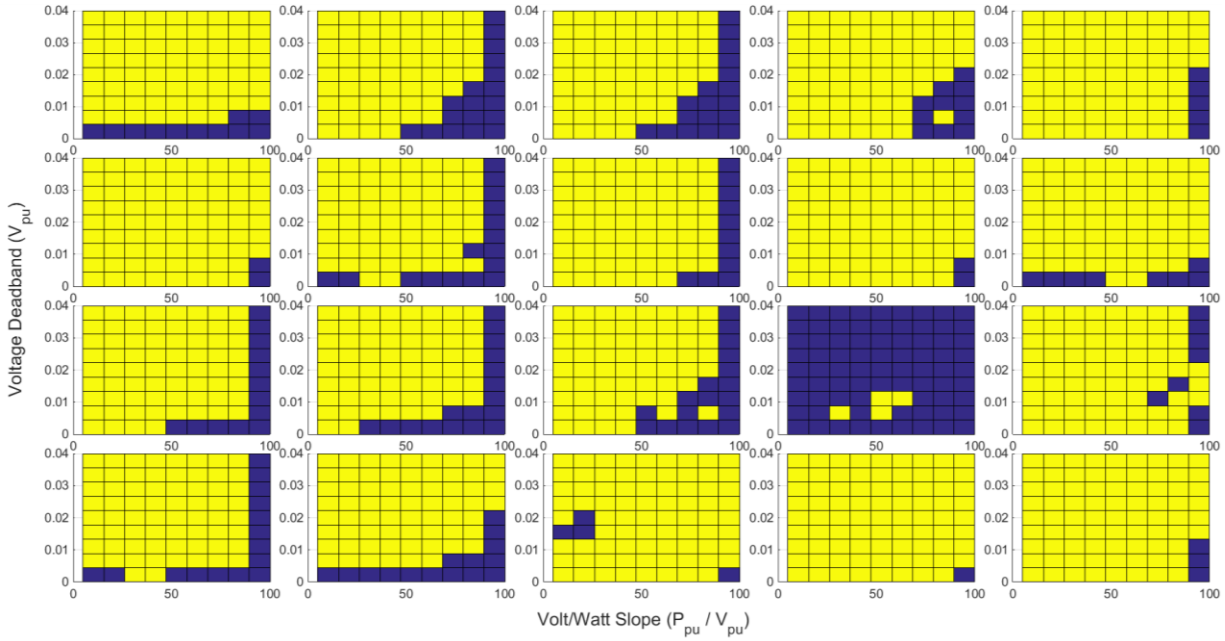

Figure 38. Control parameter regions in yellow that improve the network metrics more than the Volt/Watt control action used with no objective score biasing.

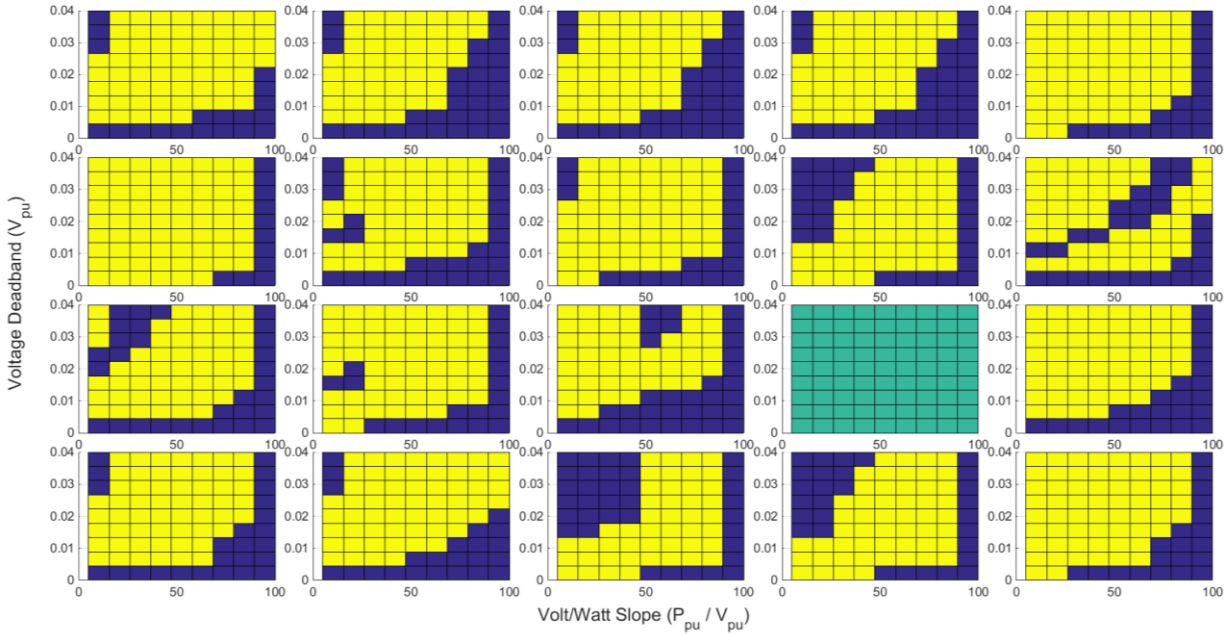

Figure 39. Control parameter regions in yellow that improve the network metrics past a bias of -1.0 added to (1) to highlight the impact of the Volt/Watt control action used.

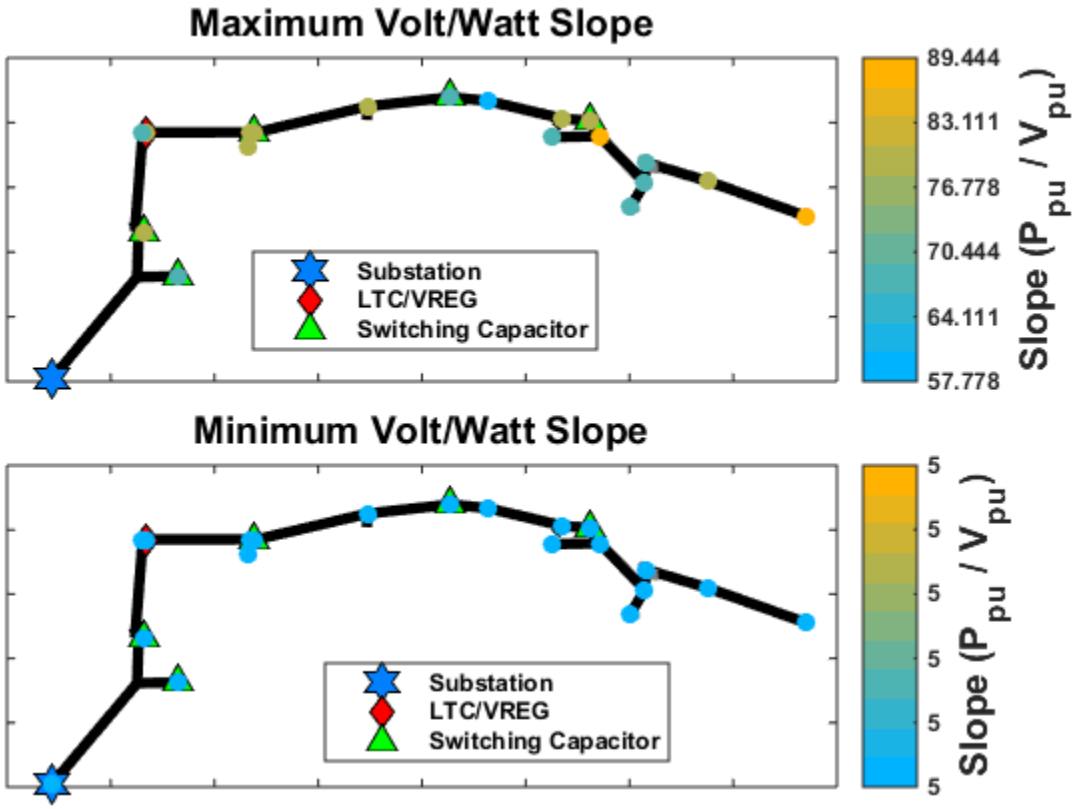

Figure 40. Volt/Watt slope upper and lower boundaries for feeder CO1 based on objective score.

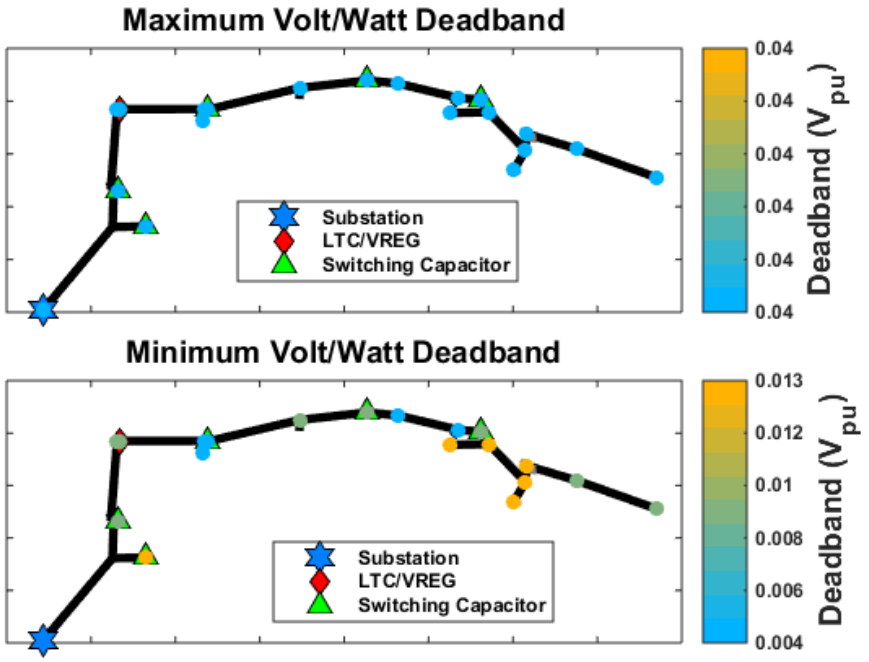

Figure 41. Volt/Watt deadband upper and lower boundaries for feeder CO1 based on objective score.

4.4. Watt-Triggered Power Factor Control

For watt-triggered power factor control, the inverter increases its var absorption based on its real power output. Figure 42 shows how the normalized network metrics vary with the two parameters that determine this control action: the target power factor at full rated output and the deadband of output power at which the control begins. While low deadband values will cause more overall control action, high deadband values will cause more aggressive var compensation. For this reason, the control settings in Figure 42 with low target power factors and high deadbands cause sharp changes in the network, resulting in more regulator and capacitor switching and under-voltages. Lower power deadband settings improve the network parameters more in general, at the cost of more reactive power use and increased network losses.

This cost only slightly skews the objective function scores to higher deadband settings since these metrics have low weights, as seen in Figure 43. A bias of 0.5 is added to (1) to compensate. The parameters that minimize the objective function are highly dependent on interconnection location with this control. Some interconnection locations have few control parameter combinations that give an overall improvement that outweighs the control cost, so in this case a positive bias of 0.5 is added to the objective function (1). This dependence can be seen clearer in Figure 45, which shows the control parameter regions that achieve a net improvement past the bias in yellow for each PV interconnection location. The upper and lower bounds of the control parameters that maximize these regions are shown in Figure 46 for target power factor and Figure 47 for power deadband. Target power factor is more location dependent on its upper bound because generally more var compensation will give greater overall network improvement with the chosen weights.

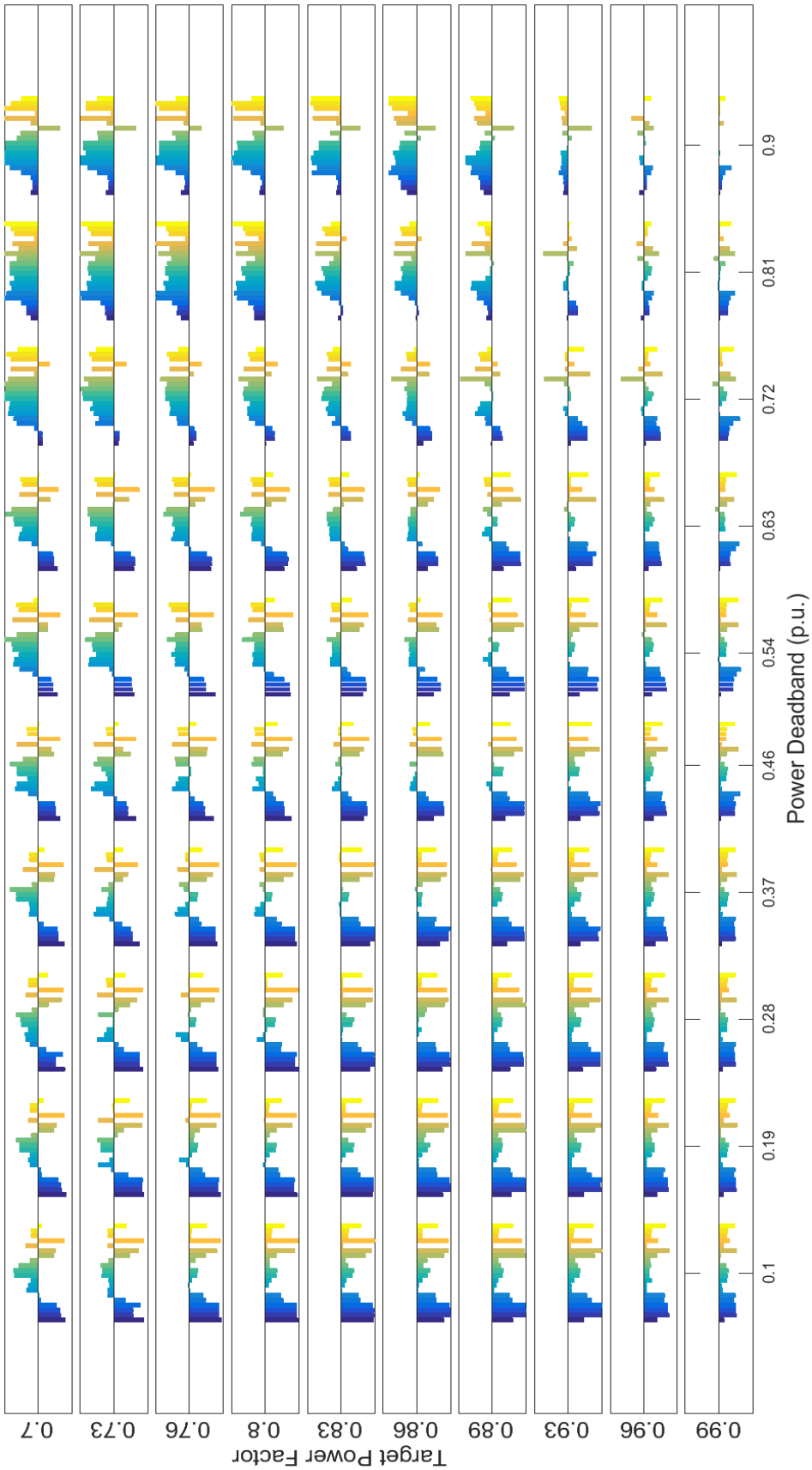

Figure 42. Sum of normalized network metric scores for each watt-triggered power factor control parameter at all PV locations.

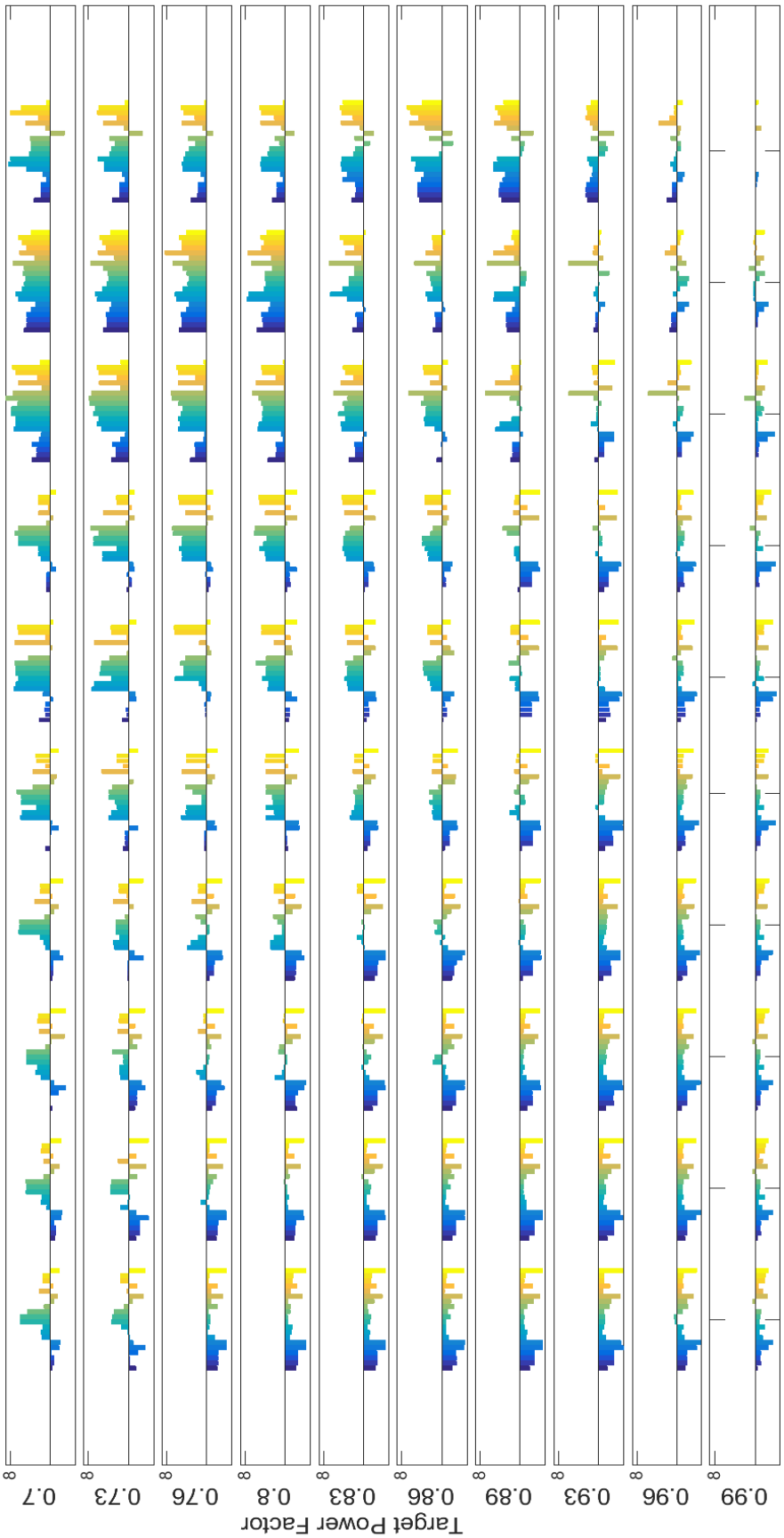

Figure 43. Objective function score for each set of watt-triggered power factor control parameters at all PV locations.

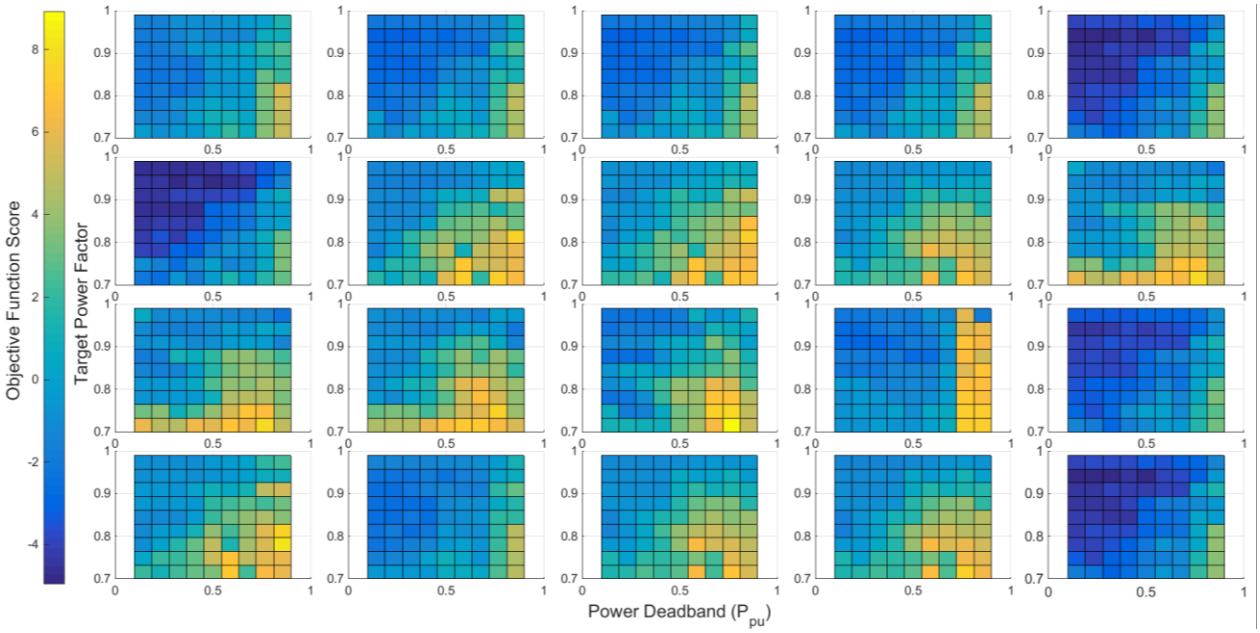

Figure 44. Watt-triggered power factor control objective function score surfaces at each PV location.

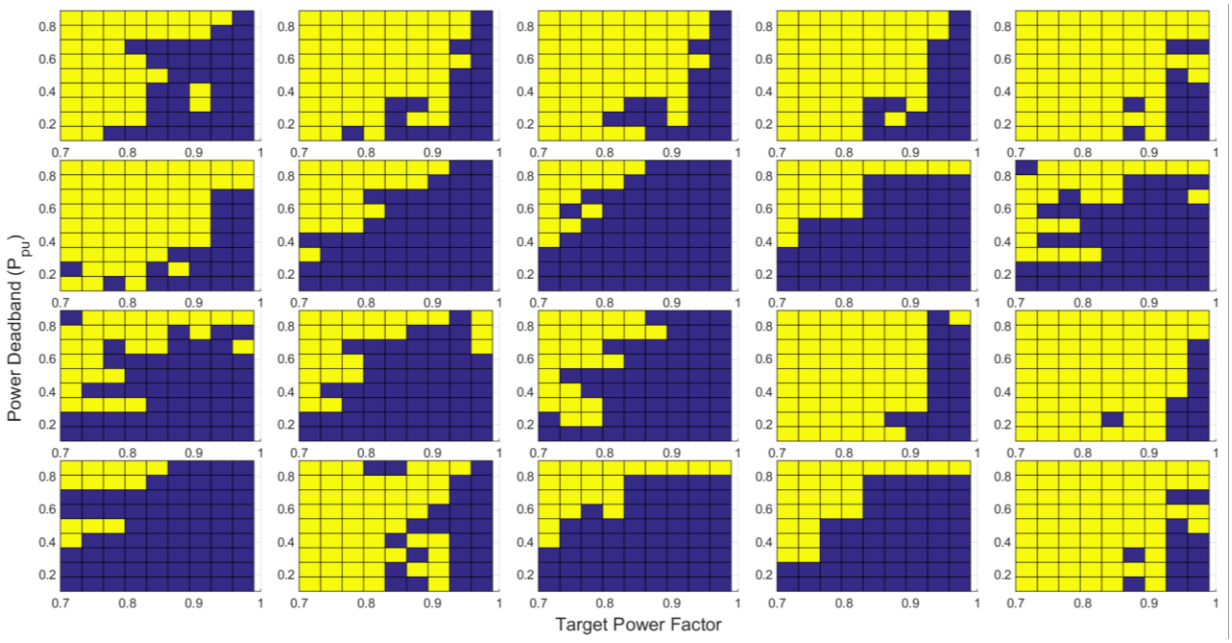

Figure 45. Control parameter regions in yellow that improve the network metrics using watt-triggered power factor control with a bias in (1) of 0.5.

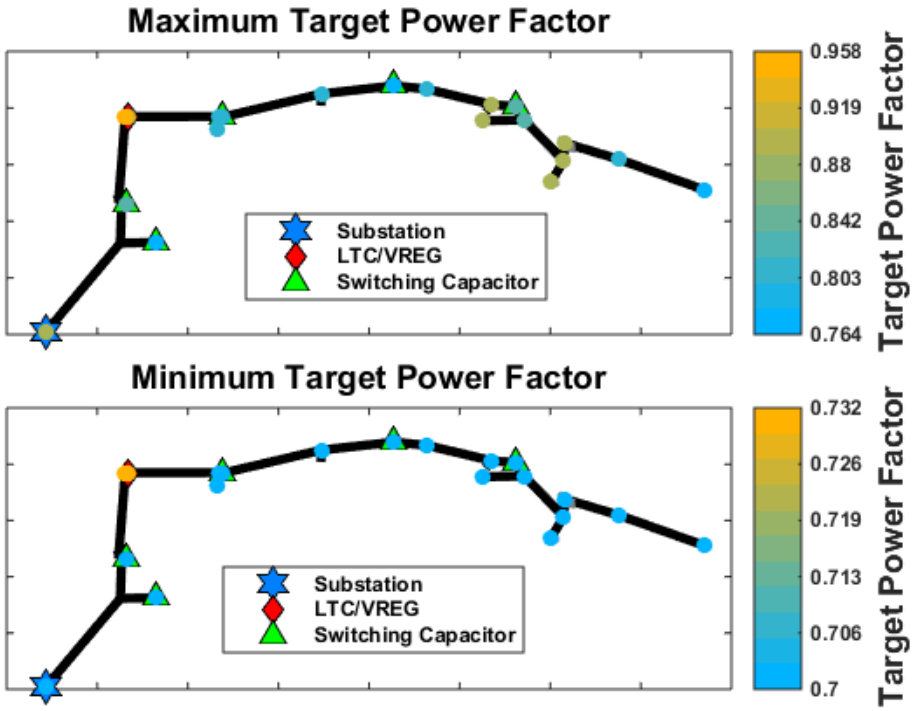

Figure 46. Upper and lower bounds of target power factor for watt-triggered power factor control for each PV interconnection in feeder CO1.

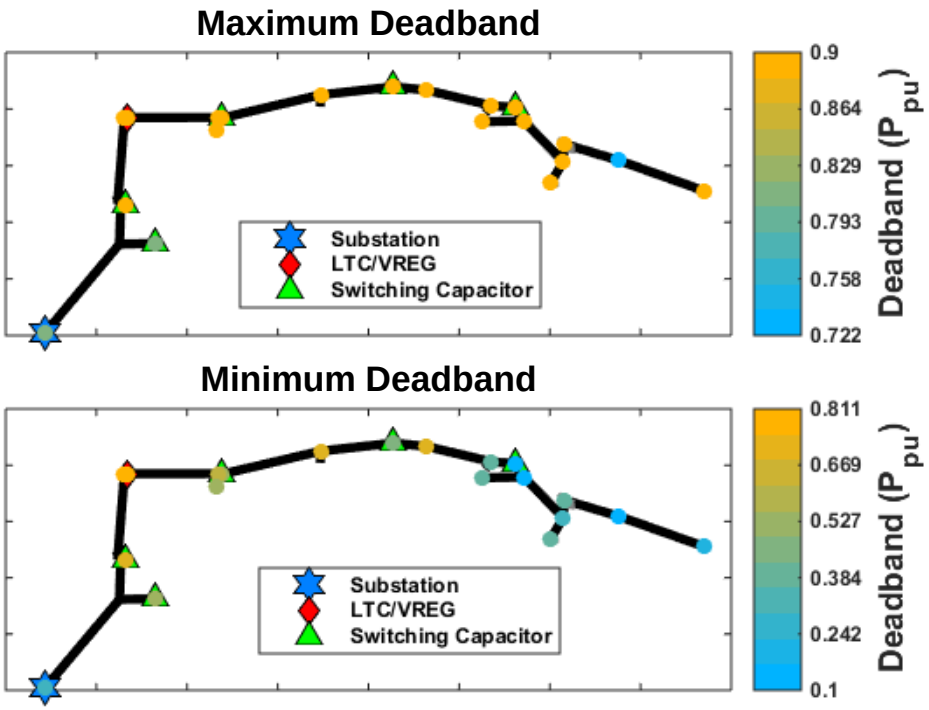

Figure 47. Upper and lower bounds of PV power output deadband for watt-triggered power factor control for each PV interconnection in feeder CO1.

4.5. Watt-Priority Volt/Var Control

Unlike the other advanced inverter controls, Volt/Var control has three parameters that may be set. This makes it difficult to visualize how the parameters impact the network metrics due to the extra dimension. This control was applied to 20 locations in feeder CS1. The normalized network metrics at each control parameter combination across the feeder is shown in Figure 48. Each of the 100 plots in this figure has a horizontal axis that represents that variation of the nominal voltage parameter. The slope parameter is then varied vertically across plots and the deadband parameter is varied horizontally across plots (viewing the figure in a landscape format). The best performing parameters are then those that produce the most negative bars across all locations, which are differentiated by color. The general trend is that network metrics improve as the Volt/Var curve slope is increased but at some point a deadband must be added to gain more improvements. Increasing the deadband of the curve too high will prevent the controller from acting enough. Therefore, the best improvements are seen at a high Volt/Var slope, say greater than $50Q_{pu}/V_{pu}$, with a deadband with a width less than $0.02V_{pu}$ but greater than $0.01V_{pu}$. In this range, using a nominal voltage around $1.0V_{pu}$ will see the greatest improvements across the feeder.

The objective function surfaces per location are too difficult to display with more than two control parameters, but the ranges of good parameter settings can still be found by the same method described in Section 3.5. The range of good Volt/Var slope values per interconnection location on feeder CS1 is shown in Figure 49, deadband ranges are shown in Figure 50, and nominal voltage ranges are shown in Figure 51.

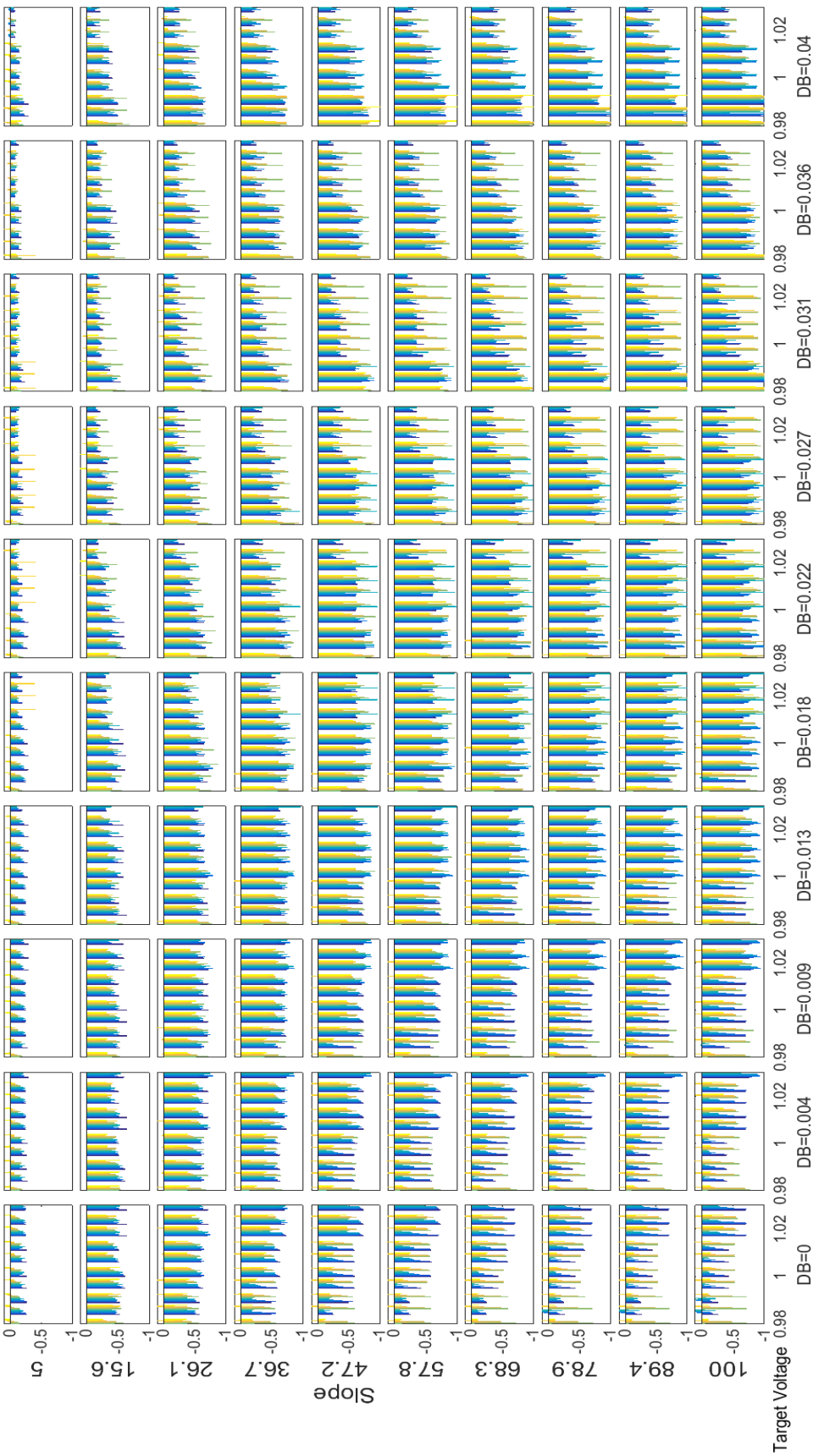

Figure 48. Normalized metric score for various Volt/Var controls applied at 20 locations in feeder QS1.

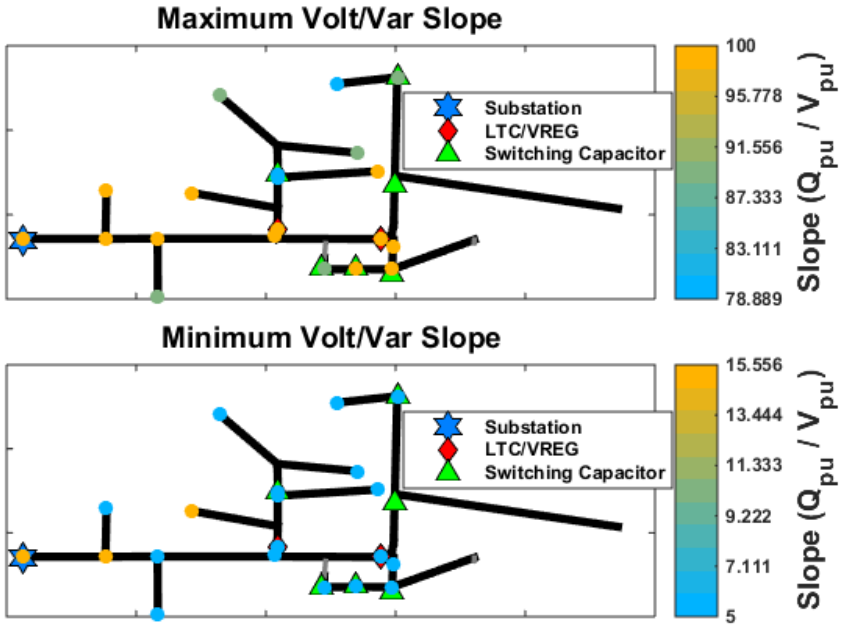

Figure 49. Upper and lower bounds of Volt/Var slope for Volt/Var control for each PV interconnection in feeder QS1.

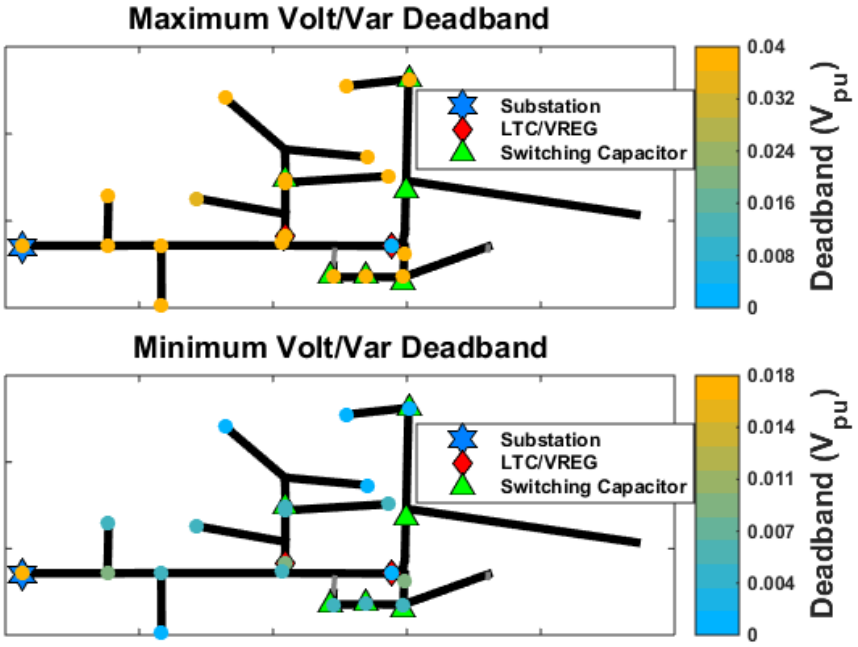

Figure 50. Upper and lower bounds of voltage deadband for Volt/Var control for each PV interconnection in feeder QS1.

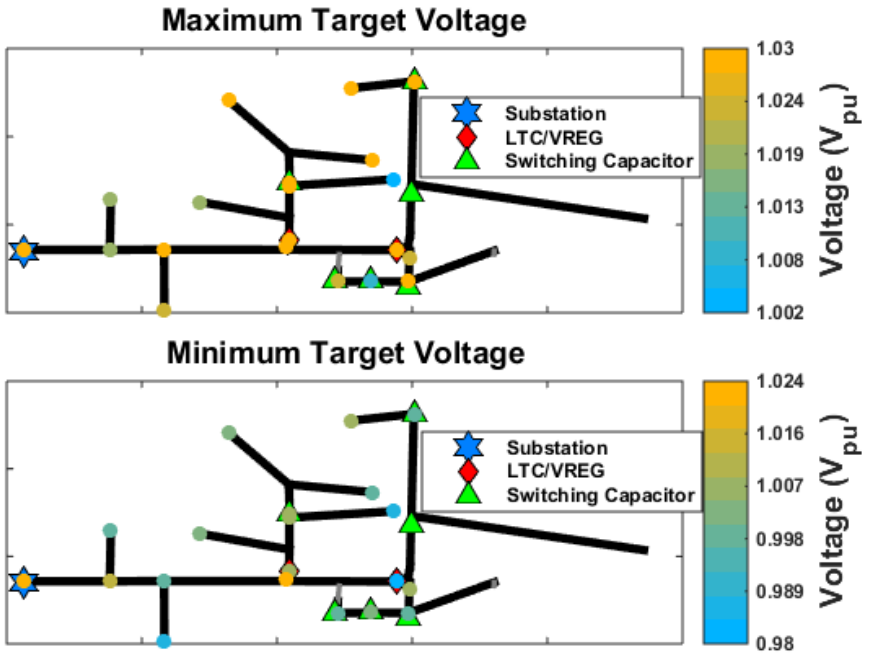

Figure 51. Upper and lower bounds of target nominal voltage for Volt/Var control for each PV interconnection in feeder QS1.

4.6. Var-Priority Volt/Var Control

Unfortunately, there are no parametric simulation results for the var-priority volt/var control type. At the time of running these simulations, a var-priority volt/var mode did not exist in the OpenDSS platform and the var-priority controls demonstrated in Section 2.2.3 were developed by communicating between OpenDSS and Matlab iteratively. This process slowed down the simulation of each one-week QSTS, as can be seen in Figure 23, compared with the other control types. Since this control type also has three parameters, running a comparable parametric study on it would have taken months to complete, which was deemed impractical.

5. GENRALIZED CONTROL SETTINGS FOR EXAMPLE FEEDERS

This section presents the method for finding the set of parameters for each control type that work well across all interconnection locations studied in the two feeders presented in Section 3.1. Each feeder has 20 interconnection locations, except for technical reasons feeder CO1 only tested the impact of Volt/Var control at four locations. To find the control settings that work well at any general location in a feeder, the binary network improvement mask, such as those shown in Figure 38, is found for the entire feeder. This is accomplished by applying the AND operator to all binary masks, which each represent an interconnection location, to get one binary mask for the entire feeder. Then, the same procedure presented in Section 3.5 is applied to find the largest area of parameter ranges that will work for the entire feeder. The general control setting ranges that work on the two feeders tested are presented below for each control type in Table 1 through Table 5.

Table 1. Ramp rate limit control parameter ranges that work across all tested locations per feeder.

FEEDER	RAMP RATE (P_{pu}/h)
CO1	0.334 – 1.50
CS1	0.667 – 1.17

Table 2. Constant power factor control parameter ranges that work across all tested locations per feeder.

FEEDER	PF
CO1	0.83 – 0.99
CS1	0.80

Table 3. Volt/Watt control parameter ranges that work across all tested locations per feeder.

FEEDER	SLOPE (P_{pu}/V_{pu})	DEADBAND (V_{pu})
CO1	5.0 – 68.3	0.01 – 0.04
CS1	5.0 – 15.6	0.009

Table 4. Watt-triggered power factor control parameter ranges that work across all tested locations per feeder.

FEEDER	PF	DEADBAND (V_{pu})
CO1	0.70 – 0.80	0.72
CS1	0.96 – 0.99	0.19 – 0.72

Table 5. Watt-Priority Volt/Var control parameter ranges that work across all tested locations per feeder.

FEEDER	SLOPE (P_{pu}/V_{pu})	DEADBAND (V_{pu})	NOM. VOLTAGE (V_{pu})
CO1*	15.5 – 100	0 – 0.022	0.997 – 1.03
CS1	15.5 – 47.2	0.018 – 0.027	1.019 – 1.03

**Represents the parameters the work well across only four test locations.*

In the above analysis, outlying data was rejected from locations that showed a poor response to control actions at over 50% of the tested settings. The data was rejected to show parameter ranges more representative of the entire feeder. Locations that do not see improvements from advanced inverter controls indicate interconnecting PV already has an overall improvement, and

these locations are not good candidates for advanced inverter controls. In Table 1, Feeder CO1 had three bad locations, and Feeder CS1 had eight. In Table 2, only Feeder CS1 had four rejected locations. But, even with rejecting outliers, only one power factor remained viable for all other locations on CS1. This indicates that there are some regions of Feeder CS1 that benefit more from differing levels of reactive power support. For example, the power factor range accepted by all of only the first 12 interconnections is $pf = [0.70 - 0.83]$. The remaining eight interconnections have much more sporadic acceptable ranges, which if included will reduce the allowable settings to only the one shown in Table 2. The conclusion is that PV interconnections are much more sensitive to interconnection location in Feeder CS1 than in Feeder CO1.

The ranges in Table 3 correspond to the binary masks shown in Figure 39, from which one can quickly visualize the single outlier location that had to be removed to achieve these parameter ranges. For Feeder CS1, the interconnection locations again greatly influence how the controls impact the network. Five locations in Feeder CS1 towards the end of the feeder had to be rejected to get the ranges in Table 3. If only the first nine interconnection locations are considered, the largest range of slopes would be $[15.6 - 57.8]$, and the range of deadbands would be $[0.013 - 0.036]$.

The ranges given in Table 4 for Feeder CO1 represent the objective function scores presented in Section 4.4, which used an objective function score bias of 0.5. This was not selected with the entire feeder in mind, however, so if it is arbitrarily increased to 1.0, the ranges of generalized parameters increases. At a bias of 1.0, the target power factor can be within $0.70 - 0.76$, and the deadband can be within $0.63 - 0.90$. For Feeder CS1, a new bias of 1.0 is selected to achieve the range of parameters shown. It is interesting to note such a difference in the selected parameters between the two feeders.

6. CONCLUSIONS AND FUTURE RESEARCH

This research presented a parametric study of various proposed advanced inverter control types acting on realistic distribution feeder models over a one week time-domain simulation. Several measurable network quantities are identified to be used as metrics to determine the effectiveness of each control. A weighted objective function is then used to score the combination of metrics against the perceived cost of control. Each control type investigated has between one and three parameters that define its time-domain behavior. These parameters are varied within a pre-determined discretized range to study how the different possible controller behaviors affect the objective function. Additionally, the PV system is tested at various locations around the distribution feeder model to study how the interconnection location impacts the effectiveness of each control type. Several approximations are made in the study to reduce its computational burden. After all the parametric studies are complete for a feeder, the largest range of parameters that satisfies the objective function is determined for each location tested, as well as those parameters that will work satisfactorily at all locations.

The first control type investigated was simply limiting the amount by which a PV system can ramp up its output to prevent problems caused by rapid irradiance transients due to clouds. Decreasing the ramp-rate limit exponentially increased the amount of PV power curtailed. Of course the greatest improvements in PV-induced network issues correspond to the highest curtailment levels, which is why power curtailment is included in scoring a control's effectiveness. The curtailment of PV power is uniform per interconnection location, but the improvements gained are highly variable between locations. This is where a careful selection in the trade-off between acceptable curtailment and desired improvement is necessary to tune the control. For the weights used in this paper, the slightest curtailment of $1.5P_{pu}/h$ scored the highest in general. However, one interconnection location did not gain any improvement with this type of curtailment.

Similar results are seen in the other curtailment control type: volt/watt control. Although there are two parameters that define this control, in general, the lower the deadband and steeper the control slope, the more the PV system will be curtailed and the more problems will be mitigated. Again, the weights were carefully selected to balance curtailment with network improvements such that the lowest objective scores across the feeder could be found around $0.02V_{pu}$ deadband and $50P_{pu}/V_{pu}$ slope. Again, the ideal parameter ranges are highly dependent on the location and certain locations result in much smaller ranges. In particular, the locations near the substation benefit most from steep slopes with large deadbands, whereas the locations near the end of the feeder benefit most from shallow slopes with shorter deadbands.

Arguably, the more interesting results are achieved with the advanced inverter controls that employ reactive power. This is because use of PV inverter reactive power capabilities are typically not viewed as negatively as real power curtailment, but there is not as clear of a connection between increased var output and decreased PV-induced issues. The simplest form of var control is constant power factor. Interestingly, the network improvements increased with lower power factor (more var output) up to 0.89 lagging before falling off and actually starting to increase overall network problems at around 0.8 lagging power factor. Watt-triggered power factor control is much more variable between interconnection locations. This is likely due to the

fact that the PV system real power output impacts the network much differently between interconnection locations. Also, if the reactive power control is triggered sooner, it generally has a better overall improvement. Large deadbands result in steeper var slopes, which in turn leads to negative interactions with existing voltage controllers. Lastly, volt/var control is much more difficult to generalize due to the additional parameter dimension. However, it is the control that has the most overall improvement at the largest number of parameters. Only the steepest control slopes with the smallest deadbands, which correspond to the most aggressive control behaviors, actually result in more negative impacts on the network. In general, keeping a gradual slope around $50.0 Q_{pu}/V_{pu}$ with a deadband with a width of at least $0.01 V_{pu}$ seems to lead to the most improvements across the feeder. After that, it seems larger deadband settings correspond positively to lower nominal voltages, and vice versa.

In general, since there is an inherent conflict between control action and network improvements, the weighting and biasing of the objective function heavy impacts the results. The parameter ranges presented in this paper would be skewed by different weights and biasing. Additionally, it has been shown that the interconnection location of the PV system plays a significant role on the impact an advanced inverter control may have. This is corroborated by past research that has shown that the PV interconnection location can largely determine if it will cause any negative impact at all on the feeder. Lastly, at the publishing of this report, it has been discovered that the OpenDSS PV system QSTS simulation platform had a bug that may have altered the outcome of some of the many simulations presented here. For these reasons, reproduction of the studies presented in this report may yield different numerical results. The scope of this research is to present a method by which certain parameter settings may be ruled out or find locations ill-suited for certain control types may be identified, not to suggest the use of specific control parameters for an advanced inverter controller.

To continue this research, further analysis should be made on the additional distribution feeder models. Included in this analysis should be a review of trends across the feeder models and they correspond to aspects of the feeders. Continued research should also examine the impact of certain advanced inverter control strategies on multiple PV distributed throughout a network. Some controls may work well for a single PV system, but interactions established between neighboring PV systems due to a control could adversely impact the feeder. Additionally, rather than looking solely at potential negative impacts of the controls, future research should investigate the trade-offs that exist between network improvements and the fair control of multiple PV. This future research should conclude with a study of how these advanced inverter controls can be used to maximize the amount of PV allowed on a distribution feeder.

7. REFERENCES

[1] M. J. Reno, K. Coogan, S. Grijalva, R. J. Broderick, and J. E. Quiroz, "PV interconnection risk analysis through distribution system impact signatures and feeder zones," in *IEEE PES General Meeting Conference & Exposition*, 2014, pp. 1-5.

[2] K. Coogan, M. J. Reno, S. Grijalva, and R. J. Broderick, "Locational dependence of PV hosting capacity correlated with feeder load," in *IEEE PES T&D Conference and Exposition*, Chicago, IL, 2014, pp. 1-5.

[3] S. S. Sena, J. Q. Quiroz, R. J. Broderick, "Analysis of 100 SGIP Interconnection Studies," Sandia National Laboratories, SAND2014-4753, 2014.

[4] J. E. Quiroz, M. J. Reno, and R. J. Broderick, "Time series simulation of voltage regulation device control modes," in *IEEE 39th Photovoltaic Specialists Conference (PVSC)*, 2013, pp. 1700-1705.

[5] Y. P. Agalgaonkar, B. C. Pal, and R. A. Jabr, "Distribution Voltage Control Considering the Impact of PV Generation on Tap Changers and Autonomous Regulators," *IEEE Transactions on Power Systems*, vol. 29, pp. 182-192, 2014.

[6] B. Seal, "Standard Language Protocols for Photovoltaics and Storage Grid Integration," EPRI, May, 2010.

[7] "Recommendations for Updating the Technical Requirements for Inverters in Distributed Energy Resources," California Public Utility Commission, California Public Utility Commission, 2014.

[8] M. J. Reno and K. Coogan, "Grid Integrated Distributed PV (GridPV) Version 2," Sandia National Laboratories, SAND2014-20141, 2014.

[9] M. Lave, M. J. Reno, R. J. Broderick, "Characterizing local high-frequency solar variability and its impact to distribution studies", *Solar Energy*, Vol. 118, August 2015

[10] M. J. Reno, K. Coogan, R. Broderick, and S. Grijalva, "Reduction of distribution feeders for simplified PV impact studies," in *IEEE 39th Photovoltaic Specialists Conference (PVSC)*, 2013, pp. 2337-2342.

DISTRIBUTION

1	MS1033	Robert J. Broderick	6112
1	MS1033	Abraham Ellis	6112
1	MS1140	Matthew J. Reno	6113
1	MS1140	Ross Guttromson	6113
1	MS0899	Technical Library	9536 (electronic copy)


Sandia National Laboratories